A Study on Retention Mechanism of Recombinant Human Monoclonal Antibodies in Hydroxyapatite Chromatography

by

Taishiro Nakagawa

2010

学　位　論　文　の　要　旨

A Study of Retention Mechanism of Recombinant Human Monoclonal Antibodies in Hydroxyapatite Chromatography

（ハイドロキシアパタイトクロマトグラフィーにおける
組換えモノクローナルヒト抗体溶出メカニズムの研究）

氏名　　中　川　泰　志　郎

（１）抗体医薬はヒトが本来持つ免疫機能の一つである抗体の性質を利用した分子標的薬であり、抗体医薬作製技術の革新的進歩によりバイオ医薬品に占める割合は急激に増加している。しかしながら、現在、抗体医薬の創薬標的となるたん白質は期待されたほど多くはなく、製薬企業間の新薬開発競争が激化しているため、候補抗体について競合グループに先駆けて臨床試験を開始し、またマーケットに導入する速度が求められる。このため、抗体医薬品の製造方法開発期間を短縮化し、臨床試験を迅速に開始することによって候補抗体の価値を開発早期に判断することの意義は大きい。一方、抗体医薬によく利用されるIgG 抗体について、共通のサブクラス間では抗体構造全体の 2/3 を占める定常領域の構造はほぼ共通と考えられる。更には可変領域の骨格構造も高い相同性があることが知られている。このことから、組換え抗体医薬品の製造方法に一般的に用いられているカラムクロマトグラフィーにおいて、目的抗体の溶出挙動は、抗体タンパク質の一次構造から予測できることが期待される。この予測方法の確立は製造方法開発期間の迅速化に繋がると考えられる。本研究では、モノクローナル抗体の精製に広く利用されているハイドロキシアパタイト充てん剤に関する溶出位置予測方法の確立を目的として、抗体構造と溶出挙動の相関について、組換えモノクローナル抗体を用いての解明を試みた。

（２）ハイドロキシアパタイトはインプラント材料としての臨床応用以外にも、中性付近においてクロマトグラフィーが可能であり、かつ比較的高い特異性を有する精製用充てん剤としての利用価値がある。その分離原理には陽イオン交換作用を持つリン酸基とタンパク質表面上のカルボキシル基とのキレート結合能（金属アフィニティ結合能）を有するカルシウム基が関与し、これらの複雑な相互作用により、タンパク質の微妙な構造の違いを認識できると考えられている。カラムクロマトグラフィーにおける有効な溶出条件として、リン酸ナトリウム濃度勾配溶出及び塩化ナトリウム濃度勾配溶出条件が知られており、リン酸ナトリウム濃度勾配溶出モードにおいては、タンパク質の等電点と溶出位置に正の相

関の傾向があることが知られている。

（３）リン酸ナトリウム濃度勾配溶出条件における組換えモノクローナルヒト抗体の抗体構造と溶出挙動との相関について検討した結果、(i) 可変領域と定常領域の両方が溶出挙動に影響を与えている、(ii) 重鎖可変領域の塩基性アミノ酸の数と溶出位置に正の相関があり、抗体等電点とは相関がない、(iii) この正の相関は塩基性アミノ酸のタンパク質表面の露出度を考慮すると更に向上される（相関係数=0.87）、ことを見出した。

（４）塩化ナトリウム濃度勾配溶出条件における組換えモノクローナルヒト抗体の抗体構造と溶出挙動との相関について検討した結果、(i) 可変領域の寄与は小さく、定常領域が溶出挙動に影響を与えており、サブクラスのみからの溶出位置の分類が可能である、(ii) 溶出挙動に影響を与える相互作用機構として、金属アフィニティ結合と陽イオン交換作用が協調的に作用していることが推察される、ことを見出した。

（５）以上の結果、本研究により、組換えヒトモノクローナル抗体を用いたハイドロキシアパタイトクロマトグラフィーの溶出挙動はリン酸ナトリウム濃度勾配溶出条件、塩化ナトリウム濃度勾配溶出条件では異なり、溶出位置は抗体サブクラス、可変領域の一次構造から予測可能であることが示唆された。これらの結果を応用することにより、抗体医薬製造におけるハイドロキシアパタイトクロマトグラフィーの溶出条件の最適化について、一次構造情報のみから迅速に予測することが可能であり、効率的な抗体精製方法の開発に役立つことが考えられる。

CONTENTS

ABBREVIATIONS

MAb, monoclonal antibody

rhMAb, recombinant human monoclonal antibody

POC, proof of concept

V_H region, heavy chain variable region

V_L region, light chain variable region

C_H, heavy chain constant region

C_L, light chain constant region

Fab, fragment, antigen binding

Fc, fragment, crystallizable

CDR, complementarity determining region

PDB, Protein Data Bank

p*I*, isoelectric point

P-site, phosphate-site

C-site, calcium-site

NaPi, sodium phosphate

NaCl, sodium chloride

t_r, retention time

I.D., inside diameter

r^2, correlation coefficient

SD, standard deviation

CV, coefficient of variation

Arg, arginine

Lys, lysine

Glu, glutamate

Asp, aspartate

His, histidine

cDNA, complementary DNA

RT-PCR, reverse transcriptase polymerase chain reaction

IEF, isoelectric focusing analysis

RSA, relative side chain solvent accessibility

N-glycan, asparagine (N)-linked oligosaccharides

C_{Na}, peak sodium ion concentration by sodium phosphate gradient elution

C_{phos}, peak phosphate ion concentration by sodium phosphate gradient elution

C_{NaCl}, peak sodium chloride concentration by sodium chloride gradient elution

GENERAL INTRODUCTION

1. Monoclonal Antibody Therapeutics

Monoclonal antibody therapy (MAb therapy) is one of the molecularly-targeted therapies taking advantage of the properties of antibodies to bind specifically to the targets on the surface or exterior of host cells or invading pathogens [1–5]. The clinical trial of MAb therapy started [broke out?] with the advent of hybridoma technology developed by Köhler and Milstein in 1975 [6]. This technological innovation enabled us to produce a single, homogeneous murine antibody of predefined antigen specificity, and various therapeutic murine MAbs entered clinical trial in the early 1980s. In the next decade, the development of chimeric and humanized MAb technology (Fig. 1) reduced potential risks of immunogenicity and rapid clearance of murine antibodies in human therapy (Table 1) due to patients' production of human anti-mouse antibodies [7, 8]. Chimeric MAbs are composed of murine variable regions fused to human constant regions, and 67% of the total amino acid sequences are of human origin. Amino acid sequences of murine origin are further reduced in humanized MAbs by grafting murine hypervariable amino acid domains into human antibodies (approximately 90% human origin). Furthermore, advancements in genetic engineering techniques have finally provided fully recombinant human MAbs (rhMAbs) taking advantage of trans-chromosome and phage display technologies [9–11].

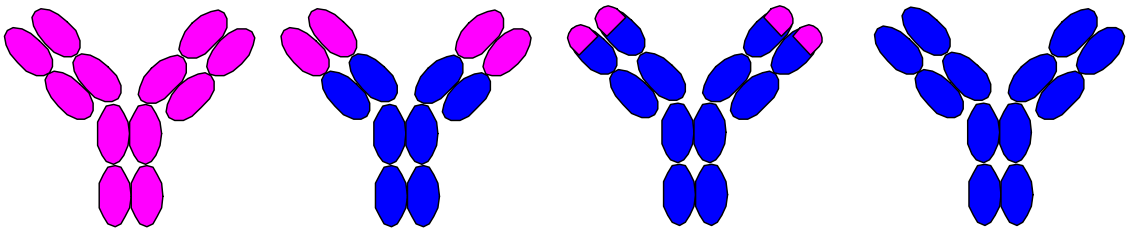

Fig. 1. Antibody engineering for humanization. Mouse- and human-derived amino acid sequences are drawn in pink and in blue, respectively. The percentages described below each antibody type show the occupancy fraction of human derived amino acid sequence. Chimeric antibody combines the mouse variable regions with the human constant regions. Humanized antibody is produced by CDR-grafting technology, and the variable regions consist of antigen binding CDRs of mouse origin in association with human framework regions.

Table 1.

Incidence of antibodies in humans administered monoclonal antibody drugs

Antibody drug	Antibody type	Incidence
Oncoscint (anti-TAG)	mouse IgG_1	55%
OKT3 (anti-CD3)	mouse IgG_{2a}	~80%
Rituxan (anti-CD20)	chimeric IgG_1	< 1%
Simulect (anti-IL2Ra)	chimeric IgG_1	< 2%
ReoPro (anti-GPIIb/IIIa)	chimeric IgG_1 Fab	7-19%
Remicade (anti-TNF)	chimeric IgG_1	10-57%
Erbitux (anti-EGFR)	chimeric IgG_1	5%
Synagis (anti-RSV)	humanized IgG_1	< 1%
Herceptin (anti-HER2)	humanized IgG_1	0.1%
Zenapax (anti-IL2Ra)	humanized IgG_1	8%
Campath (anti-CD52)	humanized IgG_1	< 2%
Avastin (anti-VEGF)	humanized IgG_1	None detected
Humira (anti-TNF)	human IgG_1 (phage)	> 5%

Source: E. Koren et al. [8]

2. Heated competition in a growing market of MAb therapy

Currently, therapeutic MAbs are the second largest biopharmaceutical product category after vaccine (Fig. 2), and the current pipelines of therapeutic MAbs in clinical trial contain more than 160 products in 2006 in the United States [12, 13]. This means that the MAb products for human therapies account for over 30% of biopharmaceuticals in clinical trials [12, 13]. However, at the present time, the number of target antigens available for MAb therapy is limited. Moreover, because substance patents of some target antigens are ambiguous in the application for antibody therapies, several biopharmaceutical companies are concurrently developing different MAb products for the same antigens. For these reasons, biopharmaceutical companies must assess the true clinical and commercial potentials (POC, proof of concept) of their products as early as possible. Thus, shortening of the research and developing period for their target products before commencing clinical trials is a key factor to compete in the growing market.

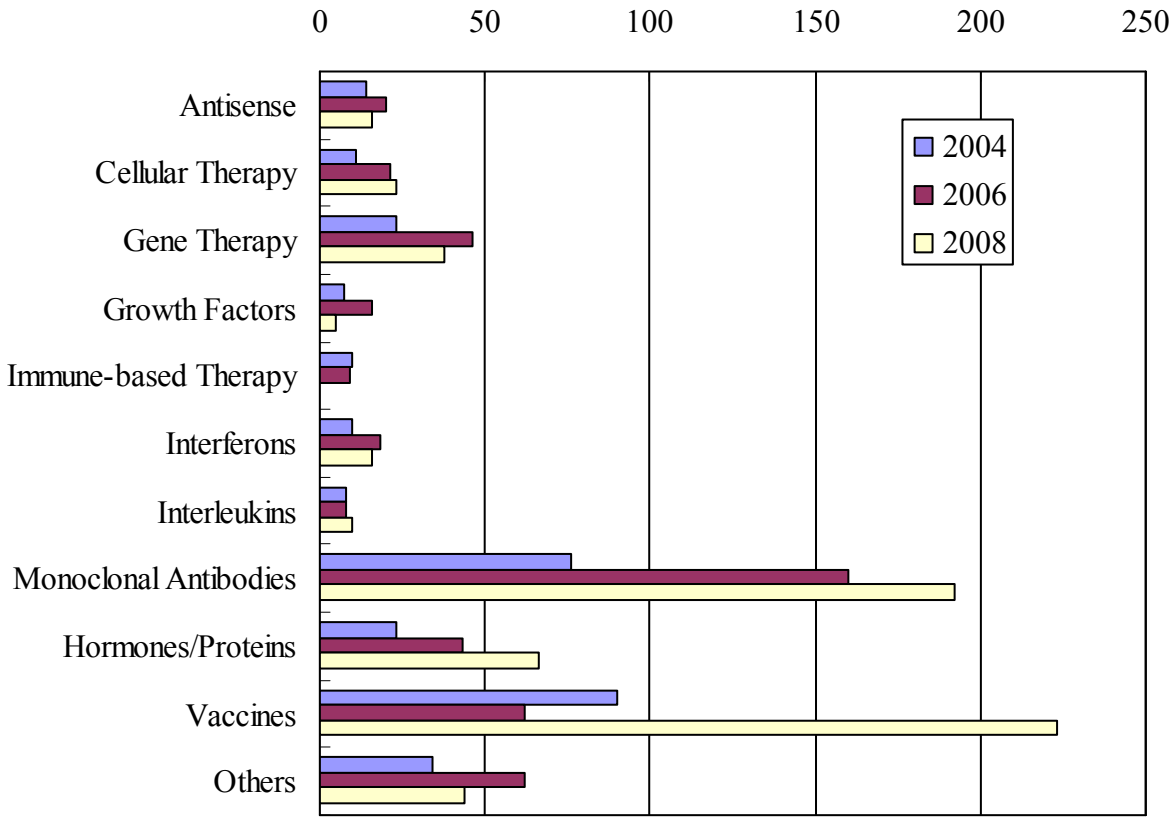

Fig. 2. Comparison of the number of biotechnology medicine pipelines between 2004 and 2008.

Source: PhRMA [12, 13].

3. Structure of antibodies

In most higher mammals, antibodies exist in five distinct classes (IgG, IgA, IgM, IgD and IgE), which differ both in form (size, charge, amino acid composition, carbohydrate content) and functions [14]. Each antibody of the five classes consists of functional units of Y-shaped and bifunctional molecules with a basic symmetrical structure (Fig. 3), and each unit consists of four polypeptides: two identical light and two identical heavy chains. Each heavy chain has two regions: the constant region (C_H region) and variable region (V_H region) [15]. The subclass of an antibody is determined by the type of the C_H region. The C_H region is identical in all antibodies of the same subclass isotype, but differs in antibodies in different subclass isotypes. On the other hand, an antibody structure can be classified into two identical Fab (Fragment, antigen binding) and one Fc (Fragment, crystallizable) fragments by their unique functions [15]. These fragments are connected by the hinge region, which contributes the flexibility of the antibody molecule.

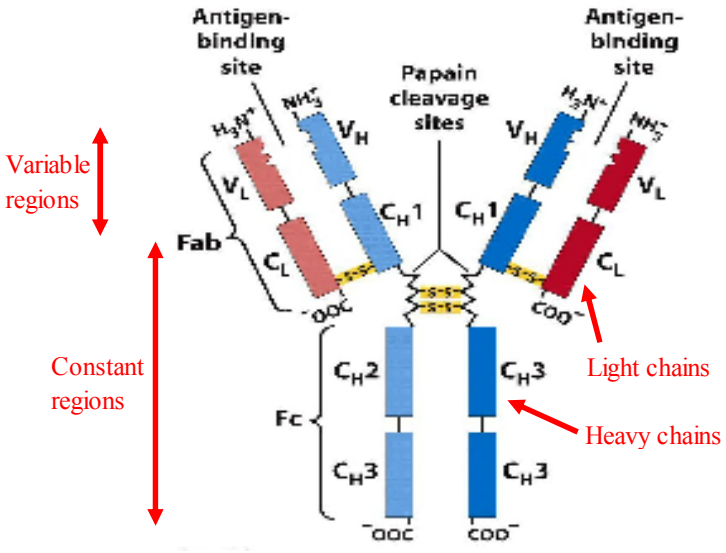

Fig. 3. Schematic structure of a functional unit of antibodies. Heavy and light chains are folded into domains, each containing about 110 amino acids and an intra-chain disulfide bond that forms a loop of 60 amino acids. V_H, heavy chain variable region; V_L, light chain variable region; C_H, heavy chain constant region; C_L, light chain constant region; CHO, glycoform.

Source: Lehninger, Principles of Biochemistry, Fifth edition, 2008, [16].

IgG is adopted mainly for the human antibody therapy, and IgG antibodies have four subclass isotypes (IgG_1, IgG_2, IgG_3, and IgG_4, Fig. 4) [17]. Each of IgG subclass isotypes has various features such as stabilities and functions (Table 2), and these features are decisive in selecting the most suitable subclass for the target of the MAb therapy. IgG_3 are difficult to handle for manufacturing because IgG_3 does not bind to protein A resin, which is an affinity absorbent commonly used at the initial capture step during recombinant MAb purification [18]. In addition, the hinge region of human IgG_3

is much longer and is prone to proteolysis than are IgG_1, IgG_2 and IgG_4 [1]. Regarding IgG_4, it is well known that its interchain bonds are easily broken *in vivo* and new interchain bonds can be formed between different IgG_4 half-molecules [19–20]. To prevent the generation of such unwanted bivalent and bispecific form of IgG, IgG_4P mutated form (Ser228Pro, EU-index numbering scheme [21]) was developed, which is useful for MAb therapy [22]. The IgG_4PE mutated form (Ser228Pro and Leu235Glu) is also used to reduce the antibody-dependent cellular cytotoxicity [23]. Thus, concurrently, IgG_1, IgG_2 and IgG_4 mutated form (IgG_4P or IgG_4PE) make up the major part of MAb therapeutic applications. On the other hand, light chains can also be divided into the constant region (C_L region) and variable region (V_L region). In mammals, there are two types of light chain, which are called κ and λ light chain.

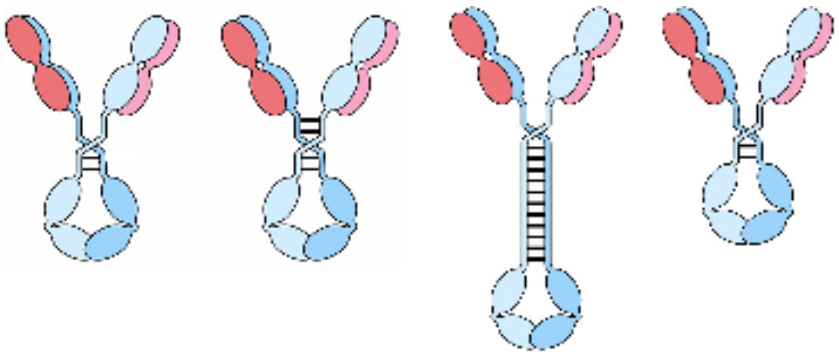

Fig. 4. Schematic diagram of the four subclasses of human IgG. Black bar represents inter-chain disulfide bond.

Table 2.

Biological properties of the four human IgG subclasses

Isotype	IgG_1	IgG_2	IgG_3	IgG_4
Molecular weight	150,000	150,000	150,000	150,000
Hinge amino acid number	15	12	62	12
Interchain disulfide bond number	2	4	11	2
In vivo serum half life (days)	21–23	20–23	7–8	21–23
Complement fixation	++	+	+++	–
Monocyte FcRI receptors binding	+++	–	+++	+
FcRII receptors on neutrophilis and eosinophilis binding	+++	+	+++	+
monocyte FcRIII receptors binding	++	–	++	–
Protein A binding	+++	+++	–	+++

Strong binding +++, medium interaction ++, weak interaction +, no interaction –

A number of 3D structural data of human Fab fragments can be obtained from the protein structural database, Protein Data Bank (http://www.rcsb.org/pdb/). According to the comparison analysis using these 3D structural data, Honneger et al. showed the high conservation of the basic folding pattern and the core positions (Fig. 5) [24]. Besides, 3D structural information of several IgG_1 Fc fragments and one entire human IgG_1 MAb (PDB code: 1HZH) can be obtained from the same database (Fig. 6). However, at the present time, there is limited 3D structural information for the Fc regions of IgG_2 and IgG_4.

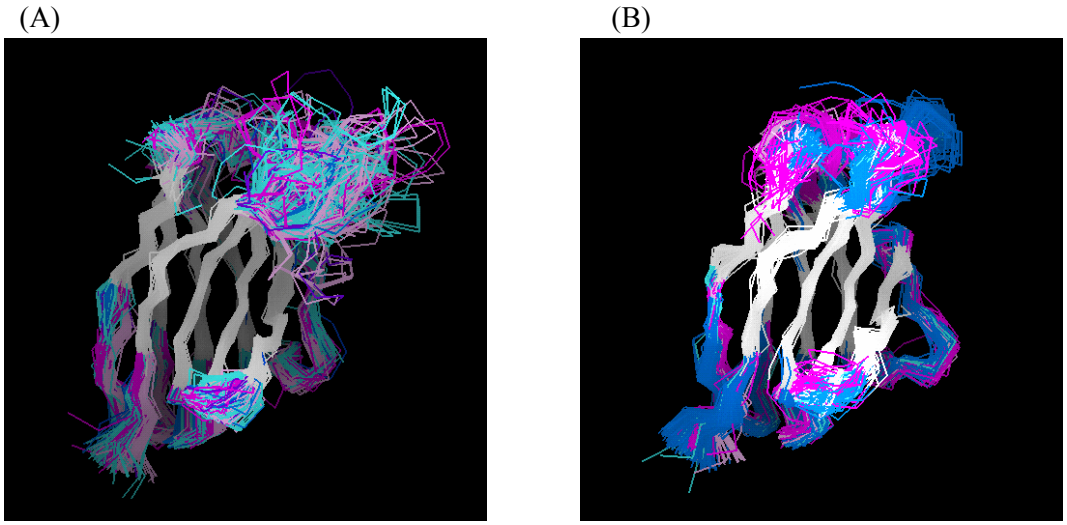

Fig. 5. Overlay of the 3D structures of various human IgG variable regions obtained from the PDB database. (A), heavy chain; (B), light chain. Source: A. Honneger et al. [24].

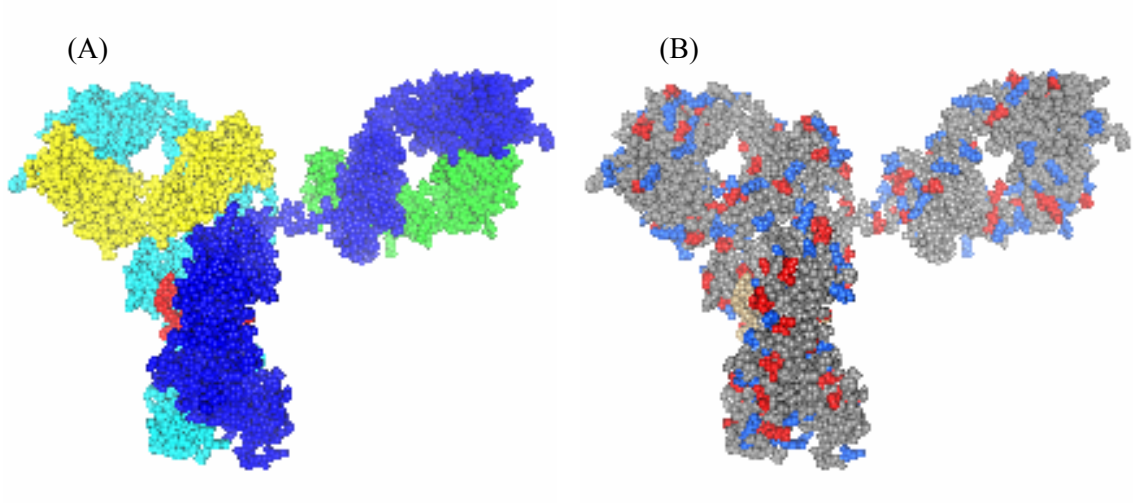

Fig. 6. Crystal structure of the recombinant human κ IgG_1 antibody which recognizes the CD4-binding site of immunodeficiency virus-1 (HIV-1) gp120 (PDB code: 1HZH) [25]. The overall shape is between Y and T, with a 143° angle between the major axes of the two Fab regions.

4. Platform approach for the rapid establishment of production process

Because of the high molecular similarities of antibodies (Figs. 4, 5), in modern production process development of MAb products, process trains are expected to be compiled with generic modules that are pre-developed at scale rather than designed de-novo for every new product, in order to introduce target products into clinical trials in the shortest time possible [14]. This generalized strategy of production process development for every MAb product is called a platform approach [26, 27]. The advantage of this approach of purification process is that suitable combinations of chromatography steps are determined beforehand and minimal chromatography experiments are performed to determine details of the purification conditions. However, to establish an efficient platform for purification scheme, it is necessary to clarify the relation between retention behavior in each chromatography step and the physicochemical properties of MAb proteins. In particular, reliable prediction of the retention behavior by easily obtainable information of the target products such as amino acid sequences or isoelectric point values (p*I* values) will be useful for the rapid establishment of the purification scheme [28, 29].

5. Hydroxyapatite

Hydroxyapatite is a basic calcium phosphate which has the chemical formula $Ca_{10}(PO_4)_6(OH)_2$, and is most stable phase of calcium phosphates under ordinary conditions [30, 31]. It has been widely utilized as not only bone cements, bone replacements materials, and drug carriers but also adsorbents for liquid chromatography. Crystalline hydroxyapatite was introduced in 1956 by Tiselius et al. as the first type of hydroxyapatite adsorbent used in chromatography [32]. However, the crystallization method at that time led to the formation of unstable rectangular plate-shaped crystals, and suffered from operational limitations in chromatography such as poor flow, poor pressure resistance, and poor stability characteristics [33, 34]. This problem of fragility of the crystals was subsequently overcome by the development of ceramic-type hydroxyapatite [33–35]. Presently, the spherical and macroporous form of ceramic hydroxyapatite is widely used not only for laboratory experiments, but also for industrial applications as a powerful tool for the separation of proteins, nucleic acids, vaccine and virus [36−39].

In antibody manufacturing, hydroxyapatite chromatography stands out due to its high selectivity to remove impurities such as DNA, host-cell protein, leached protein A, and antibody aggregate forms, which are generated during MAb production processes

[35, 40, 41]. Moreover, operation of chromatography with current ceramic type hydroxyapatite has various potencies; it can be used at high flow rate to reduce the total operation time; the chromatography can be performed under neutral pH conditions; and it has high stability against the regeneration wash by high concentration solvent of sodium hydroxide. From these reasons, hydroxyapatite chromatography has been used as one of the efficient purification tools for MAbs [34, 38, 42, 43].

The adsorption mechanism of proteins to hydroxyapatite is complicated, because it involves concurrently both cationic exchange interaction and metal affinity interaction. Positively charged amino acid residues on proteins electrostatically interact with phosphate functional groups (P-sites) as cation-exchange. Metal affinity interaction is generated between calcium functional groups (C-sites) on hydroxyapatite and carboxyl clusters of proteins (Fig. 7) [35, 44–47]. In contrast, electrostatic repulsion between positively charged amino groups on proteins and C-sites, and electrostatic repulsion between carboxyl groups on proteins and P-sites also have been considered to affect the adsorption/desorption behaviors of proteins on hydroxyapatite. Furthermore, interaction between C-sites and the imidazole side chains of histidine residues has also been reported [48].

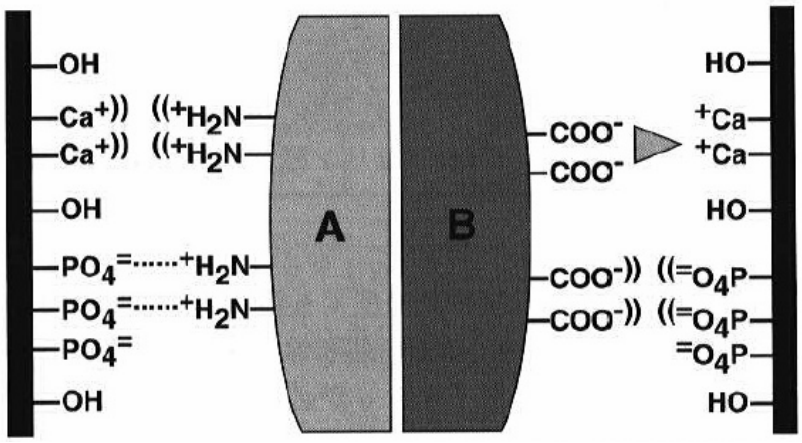

Fig. 7. Protein binding to hydroxyapatite. A is a basic protein. B is an acidic protein. Calcium ions, phosphates, and hydroxyls indicate the surface composition of hydroxyapatite. Double parentheses indicate repulsion. Dotted lines indicate ionic bonds. Triangular linkages indicate coordination bonds [35].

Antibody purification in hydroxyapatite chromatography by sodium phosphate (NaPi) gradient elution has been widely used. In the recent studies, sodium chloride (NaCl) gradient elution showed a better performance to remove unwanted impurities than NaPi gradient elution (Table 3) [40, 41]. Although NaPi gradient elution simultaneously dissociates calcium metal affinity and cation exchange interactions, NaCl gradient elution is thought not to affect calcium metal affinity interactions. Thus, some degree of phosphate ion is thought necessary for the dissociation of metal affinity interactions.

Table 3.

Comparison of contaminant clearance between NaPi gradient elution and NaCl gradient elution in hydroxyapatite chromatography of protein A purified mouse/human chimeric IgG1

Parameter	NaPi elution	NaCl elution
Aggregate	< 1%	< 1%
Leached protein A	< 1 ppm	< 1 ppm
Host cell derived protein	< 72 ppm	< 12 ppm
Host cell derived DNA	< 7 ppm	< 1 ppm
Endotoxin	< 5 EU/mL	< 0.1 EU/mL

Source: P. Gagnon et al. [41]

Regarding the retention behavior of proteins in hydroxyapatite chromatography, it is reported that retention time shows a tendency to increase with p*I* value (Fig. 8), and that the major mode of separation would be cation exchange [49, 50]. However, the selectivity is distinct from classical cation exchange. Concurrently generated repulsion between positively charged residues and C-sites, and the geometric distribution of charges on the surface of proteins must be the reason for this difference of the selectivity between hydroxyapatite chromatography and cation exchange chromatography [35]. It was also shown that the denaturation of proteins (lysozyme, cytochrome c and pancreatic deoxyribonuclease) reduces their affinity for hydroxyapatite [51]. Moreover, by the study using variants of β-lactoglobulin, it is presumed that hydroxyapatite chromatography distinguishes a slight difference in the constellation of adsorption groups on a local surface of protein molecules [52, 53].

Therefore, in order to predict the retention behavior of proteins in hydroxyapatite chromatography, not only the information obtained from the primary structure of the proteins but also information of the secondary and tertiary structure is necessary.

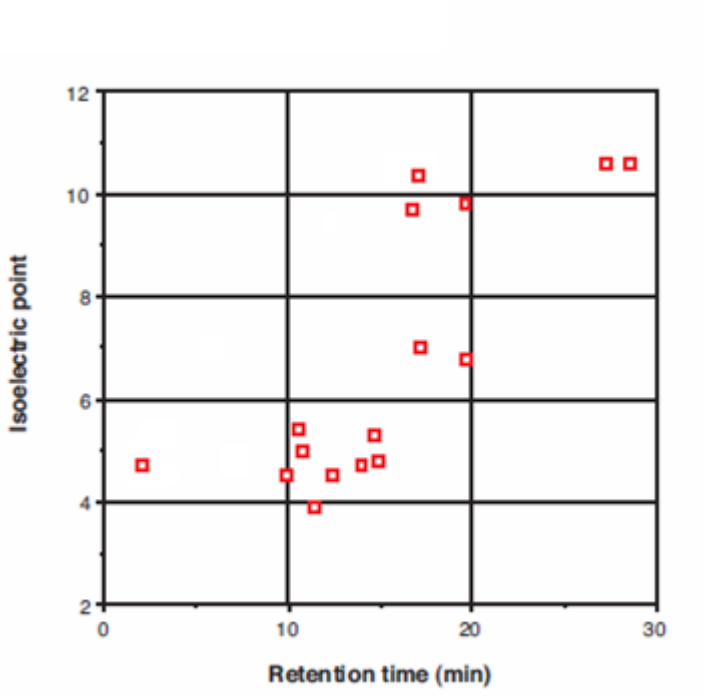

Fig. 8. Relation between the p*I* value and retention time in hydroxyapatite chromatography by NaPi gradient method for various proteins. 4.0 × 100 mm column. Linear gradient from 10 mM to 400 mM NaPi (pH 6.0) in 30 min at 0.5 ml/min [50].

6. Purpose of this study

Owing to the high similarities in IgG antibody structure, it is expected that the retention behavior of antibodies in hydroxyapatite chromatography can be predicted by the easily available information from their primary structure. The achievement of this prediction will reduce the development period in the early stage of process development for MAb therapy. In the present study, using the two elution modes generally used for hydroxyapatite chromatography, NaPi gradient elution (Chapter 1) and NaCl gradient elution methods (Chapter 2), the retention behavior of the recombinant human monoclonal antibodies (rhMAbs) were investigated. The determined retention times of the rhMAbs are discussed from the view point of the structure, particularly the electrostatic features of antibodies.

7. References

[1] P. Carter, Nat. Rev. Immunol. 6 (2006) 343.

[2] J. Reichert, C. Rosensweig, L. Faden, M. Dewitz, Nature Biotechnol. 23 (2005) 1073.

[3] P. Rohrbach, O. Broders, L. Toleikis, S. Dübel, Biotechnol. Genet. Eng. Rev. 20 (2003) 137.

[4] T. Gura, Nature 417 (2002) 584.

[5] M. Stern, R. Herrmann, Crit. Rev. Oncol. Hematol. 54 (2005) 11.

[6] G. Köhler, C. Milstein, Nature 256 (1975) 495.

[7] J. Knäblein, Modern Biopharmaceuticals: Design, Development and Optimization, Wiley-VCH, Weinheim, German, 3 (2005) 1147.

[8] E. Koren, L. Zuckerman, A. Mire-Sluis, Current Pharmaceutical Biotechnology 3 (2002) 349.

[9] K. Tomizuka, H. Yoshida, H. Uejima, H. Kugoh, K. Sato, A. Ohguma, M. Hayasaka, K. Hanaoka, M. Oshimura, I. Ishida, Nat. Genet. 16 (1997) 133.

[10] K. Tomizuka, T. Shinohara, H. Yoshida, H. Uejima, A. Ohguma, S. Tanaka, K. Sato, M. Oshimura, I. Ishida, Proc. Natl. Acad. Sci. USA 97 (2000) 722.

[11] G. Winter, A. Griffiths, R. Hawkins, H. Hoogenboom, Ann. Rev. Immunol. 12

(1994) 433.

[12] M. Miyata, Nikkei Bio Nennkan 2007, Nikkei BP, Japan, 2006, p. 39.

[13] Pharmaceutical Research and Manufacturing Association, Biotechnology Medicines Survey 2004, 2006, 2008 http://www.phrma.org/new_medicines_in_development_for_biotechnology/.

[14] J. Knäblein, Modern Biopharmaceuticals: Design, Development and Optimization, Wiley-VCH, Weinheim, German, 3 (2005) 1105.

[15] C. Janeway, P. Travers, M. Walport, M. Shlomchik, Immunobiology: The Immune System In Health And Disease (5th edition, translated in japanese), Nankodo, Japan, 2003, p. 97.

[16] D. Nelson, M. Cox, Lehninger Principles of Biochemistry (5th edition), W.H. Freeman and Company, USA, 2008.

[17] R. Jefferis, Expert Opin. Biol. Ther. 7 (2007) 1401.

[18] S. Hober, K. Nord, M. Linhult, J. Chromatogr. B 848 (2007) 40.

[19] J. Schuurman, G. Perdok, A. Gorter, R. Aalberse, Mol. Immunol. 38 (2001) 1.

[20] R. Aalberse, J. Schuurman, Immunol. 105 (2002) 9.

[21] E. Kabat, T. Wu, H. Perry, K. Gottesman, C. Foeller, Sequences of Proteins of Immunological Interest (5th edition), Public Health Service, National Institutes of

Health, 1991, p. 91.

[22] S. Angal, D. King, M. Bodmer, A. Turner, A. Lawson, G. Roberts, B. Pedley, J. Adair, Mol. Immunol. 30 (1993) 105.

[23] M. Reddy, C. Kinney, M. Chaikin, A. Payne, J. Fishman-Lobell, P. Tsui, P. Monte, M. Doyle, M. Brigham-Burke, D. Anderson, M. Reff, R. Newman, N. Hanna, R. Sweet, A. Truneh, J. Immunol. 164 (2000) 1925.

[24] A. Honegger, A. Plückthun, J. Mol. Biol. 309 (2001) 657.

[25] E. Saphire, P. Parren, R. Pantophlet, M. Zwick, G. Morris, P. Rudd, R. Dwek, R. Stanfield, D. Burton, I. Wilson, Science 293 (2001) 1155.

[26] A. Shukla, B. Hubbard, T. Tressel, S. Guhan, D. Low, J. Chromatogr. B 848 (2007) 28.

[27] L. Duncan, R. O'leary, N. Pujar, J. Chromatogr. B 848 (2007) 48.

[28] T. Ishihara, T. Kadoya, H. Yoshida, T. Tamada, S. Yamamoto, J. Chromatogr. A 1093 (2005) 126.

[29] S. Ghose, M. Allen, B. Hubbard, C. Brooks, S. Cramer, Biotechnol Bioeng. 92 (2005) 665.

[30] T. Feenstra, P. Bruyn, J. Phys. Chem. 83 (1979) 475.

[31] N. Rangavittal, A. Cánovas, J. Calbet, M. Regí, J. Biomed. Mater. Res. 51 (2000)

660.

[32] A. Tiselius, S. Hjertén, Ö. Levin, Arch. Biochem. Biophys. 65 (1956) 132.

[33] T. Kadoya, T. Isobe, M. Ebihara, T. Ogawa, M. Sumita, H. Kuwahara, A. Kobayashi, T. Ishikawa, T. Okuyama, J. Liq. Chromatogr. 9 (1986) 3543.

[34] R. Vola, A. Lombardi, M. Mariani, BioTechniques 14 (1993) 650.

[35] P. Gagnon, Purification Tools for Monoclonal Antibodies, Validated Biosystems, 1996, p. 87.

[36] S. Shepard, C. Brickman-Stone, J. Schrimsher, G. Koch, J. Chromatogr. A 891 (2000) 93.

[37] J. McCue, D. Cecchini, K. Hawkins, E. Dolinski, J. Chromatogr. A 1165 (2007) 78.

[38] A. Horenstein, F. Crivellin, A. Funaro, M. Said, F. Malavasi, J. Immunol. Methods, 275 (2003) 99.

[39] C. O'Riordan, A. Lachapelle, K. Vincent, S. Wadsworth, J. Gene Med. 2 (2000) 444.

[40] P. Gagnon, P. Ng, J. Zhen, C. Aberin, J. He, H. Mekosh, L. Cummings, S. Zaidi, R. Richieri, Bioprocess Int. 4 (2006) 50.

[41] P. Gagnon, P. Ng, J. He, J. Zhen, C. Aberin, H. Mekosh, 232th ACS National Meeting, Aneheim, CA, United States, September 10-14, 2006.

[42] C. Poiesi, A. Tamanini, A. Ghielmi, A. Albertini, J. Chromatogr. 465 (1989) 101.

[43] D. Josić, K. Löster, R. Kuhl, F. Noll, J. Reusch, Biol. Chem. Hoppe-Seyler, 372 (1991) 149.

[44] G. Bernardi, Methods Enzymol. 27 (1973) 471.

[45] M. Gorbunoff, Anal. Biochem. 136 (1984) 425.

[46] M. Gorbunoff, Anal. Biochem. 136 (1984) 433.

[47] M. Gorbunoff, S. Timasheff, Anal. Biochem. 136 (1984) 440.

[48] P. Ng, J. He, P. Gagnon, J. Chromatogr. A 1142 (2007) 13.

[49] T. Kadoya, T. Ogawa, H. Kuwahara, T. Okuyama J. Liq. Chromatogr. 11 (1988) 2951.

[50] T. Ogawa, T. Hiraide, Prep Tech '95, Industrial Separation Science Conference, East Rutherford, NJ, United States, February 13-15, 1995.

[51] G. Bernardi, T. Kawasaki, Biochim. Biophys. Acta. 160 (1968) 301.

[52] T. Kawasaki, K. Ikeda, S. Takahashi, Y. Kuboki, Eur. J. Biochem. 155 (1986) 249.

[53] T. Kawasaki, M. Niikura, Y. Kobayashi, J. Chromatogr. 515 (1990) 91.

CHAPTER 1

Relationship between human IgG structure and retention time in hydroxyapatite chromatography with sodium-phosphate gradient elution

1.1. Summary

The aim of this study was to classify the retention time of recombinant human monoclonal antibodies (rhMAbs) in hydroxyapatite chromatography with sodium-phosphate gradient elution according to their physicochemical properties. We analyzed 37 rhMAbs and found that (1) the structures of both the constant and variable regions affected retention time, (2) the number of basic amino acid residues in the variable region, particularly in the heavy chain, correlated well with retention time, and (3) this correlation was more pronounced (e.g. $r^2 = 0.87$ for 18 κ IgG_1 rhMAbs) when the surface accessibility of those residues are taken into account. These findings provide a useful guide for investigators and purification-process developers working with monoclonal antibodies.

1.2. Introduction

Hydroxyapatite chromatography [1] has been used for several decades in the purification of proteins and has recently been applied as an efficient purification tool for the manufacture of therapeutic monoclonal antibodies (MAbs) because it shows high selectivity and can be performed under neutral pH conditions [2–7]. The adsorption mechanism of proteins to hydroxyapatite is complicated [8−11]. Positively charged amino acid residues on proteins interact electrostatically with phosphate functional groups of hydroxyapatite (P-sites) via cation exchange. The adsorption mechanism also involves a metal-affinity interaction between carboxyl clusters on proteins and calcium functional groups of hydroxyapatite (C-sites). Whereas interactions via P-sites can be eliminated by an increase in ionic strength of the mobile phase, displacers such as phosphate or citrate ions are required for the dissociation of the metal-affinity interaction via C-sites. The interaction between C-sites and the imidazole side chains of histidine residues has also recently been discussed [12].

With respect to the relation between adsorption/desorption behavior of antibodies and their structures, chromatographic studies with various mouse MAbs have revealed the ability of hydroxyapatite to separate IgG idiotypes [13, 14]. With the use of a 96-well plate screening system, Wensel et al. showed that the binding strength of 15

humanized IgG MAbs to hydroxyapatite varied widely, and that IgG_2 MAbs exhibited the least overall binding compared to IgG_1 and IgG_4 MAbs [6]. Additionally, Schubert and Freitag showed using a recombinant human κ IgG_1 antibody that electrostatic interactions via Fab (fragment, antigen binding) regions play an important role in the absorption to hydroxyapatite [15]. Gagnon et al. showed that papain-digested Fab regions of a chimeric monoclonal antibody failed to bind to the calcium-derivatized hydroxyapatite [16]. An understanding of the physicochemical properties of proteins and how they relate to the retention mechanisms of chromatographic methods would provide a valuable aid for the development of purification methods [17–19]. However, the understanding of retention behaviors of MAbs in hydroxyapatite chromatography according to their structural properties is still under way.

Reliable prediction of the retention time or the peak salt concentration in column chromatography purification according to readily obtained information, such as the amino acid sequence of target MAbs, can serve as a guide for the optimization of loading and elution buffer conditions as well as the estimation of purity, which will facilitate the development of purification processes [17, 20–23]. In particular, because of the high similarities in protein structure of antibodies [24, 25], it is expected that useful parameters for the prediction of retention time of target MAbs will be identified.

Ishihara et al. reported that the retention behavior of human IgG MAbs on an SP-Sepharose FF column correlated well with the surface positive charge distribution of the heavy chain variable regions (V_H regions) and also showed that retention behavior did not depend on subclass [17]. These results led to the establishment of a rational prediction formula for determining the NaCl concentration suitable for the elution of recombinant human MAbs (rhMAbs) [17].

In the present study, in order to classify the retention behavior of rhMAbs in hydroxyapatite chromatography by sodium-phosphate (NaPi) gradient elution according to the MAb physicochemical properties, we examined the retention times (peak sodium ion concentration: C_{Na}) of 37 rhMAbs. The determined C_{Na} values are discussed from the viewpoint of antibody structure, particularly amino acid sequence.

1.3. Experimental

1.3.1. Recombinant human monoclonal antibodies

All rhMAbs used in the present study were produced in suspension cultures of Chinese hamster ovary cells, which were transfected with vectors containing antibody genes cloned from human antibody-producing mice [26]. Protein A affinity chromatography purification of cell-culture supernatants was performed by low pH stepwise elution with the use of MabSelect or Protein A Sepharose FF columns (GE Healthcare, Buckinghamshire, UK). Further purification steps (cation-exchange, anion-exchange in flow-though mode, and/or hydrophobic chromatography) were performed as necessary to improve protein purities, which were confirmed by standard analytic methods. The buffer of the purified rhMAbs was exchanged to 5 mM NaPi (pH 6.8) with the use of Amicon Ultra-4 10K molecular-weight cutoff centrifugal filter units (Millipore, Billerica, MA, USA), and the antibody concentration was adjusted to 250 μg/mL.

The classification of the 37 rhMAbs according to their physicochemical properties is shown in Table 1.1. The IgG_3 rhMAb subclass was not analyzed in this study because IgG_1, IgG_2, and IgG_4 comprise the majority of MAbs used for therapeutic applications [27]. The 10 IgG_4 rhMAbs (MAbs A-4, B-4, C-4, D-4, and 1 to 6) are also classified

according to inserted point mutations: 3 wild-type IgG_4 MAbs, 1 IgG_4P mutated MAb, and 6 IgG_4PE mutated MAbs. The IgG_4P MAb contains an amino acid point mutation of Ser228Pro in the heavy chain of IgG_4 (EU-index numbering scheme [28] used throughout) to prevent half-antibody formation [29]. The IgG_4PE MAbs additionally contain a Leu235Glu point mutation in the heavy chain to reduce antibody-dependent cytotoxicity [30]. Twelve rhMAbs, from MAb A-1 to MAb D-4, comprise 4 sets of 3 subclass isotypes. Thus, the amino acid sequences of the light chains and V_H regions in each set are identical, but their subclass is different (IgG_1, IgG_2, IgG_4, or IgG_4PE). The MAbs D-1, D-2, and D-4 contain an *N*-glycan structure in each of the V_H regions. The 19 IgG_1 rhMAbs (MAbs A-1, B-1, C-1, D-1, and E to S) and all of the IgG_2 and IgG_4 rhMAbs are classified as κ IgG antibodies. The 4 rhMAbs from MAb T to MAb W consist of λ light chains, and these light-chain constant regions are classified as IGLC3, IGLC1, IGLC2, and IGLC1, respectively, according to the international ImMunoGeneTics (IMGT) nomenclature rules [31, 32]. The germline families of the V_H and light chain variable regions (V_L regions) for each rhMAb classified by the IMGT rules are also listed in Table 1.1.

Table 1.1.

Physicochemical properties of rhMAbs and peak retention time in NaPi gradient hydroxyapatite chromatography

rhMAb	Subclass	Type of light chain	Germline family of V_H regions[a)]	Germline family of V_L regions[a)]	Isoelectric point (p*I*)	Binding site of *N*-glycan	Peak phosphate concentration, C_{Phos} (mM)	Peak sodium ion concentration, C_{Na} (mM)[b)]
MAb A-1	IgG_1	κ	IGHV6	IGKV1	8.91	C_H2	189	308
MAb A-2	IgG_2	κ	IGHV6	IGKV1	8.54	C_H2	149	243
MAb A-4	IgG_4PE[c)]	κ	IGHV6	IGKV1	8.05	C_H2	169	275
MAb B-1	IgG_1	κ	IGHV1	IGKV4	8.91	C_H2	172	280
MAb B-2	IgG_2	κ	IGHV1	IGKV4	8.58	C_H2	121	196
MAb B-4	IgG_4PE[c)]	κ	IGHV1	IGKV4	8.10	C_H2	148	242
MAb C-1	IgG_1	κ	IGHV1	IGKV1	8.86	C_H2	155	253
MAb C-2	IgG_2	κ	IGHV1	IGKV1	8.26	C_H2	86	139
MAb C-4	IgG_4	κ	IGHV1	IGKV1	7.94	C_H2	124	202
MAb D-1	IgG_1	κ	IGHV1	IGKV3	8.54	V_H, C_H2[e)]	117	190
MAb D-2	IgG_2	κ	IGHV1	IGKV3	7.94	V_H, C_H2[e)]	61	99
MAb D-4	IgG_4	κ	IGHV1	IGKV3	7.43	V_H, C_H2[e)]	77	125
MAb E	IgG_1	κ	IGHV1	IGKV1	8.53	C_H2	149	242
MAb F	IgG_1	κ	IGHV3	IGKV1	8.95	C_H2	143	233
MAb G	IgG_1	κ	IGHV3	IGKV1	9.00	C_H2	166	271
MAb H	IgG_1	κ	IGHV3	IGKV1	8.71	C_H2	156	254
MAb I	IgG_1	κ	IGHV3	IGKV3	8.94	C_H2	177	289
MAb J	IgG_1	κ	IGHV3	IGKV6	8.83	C_H2	153	250
MAb K	IgG_1	κ	IGHV3	IGKV6	8.73	C_H2	169	275
MAb L	IgG_1	κ	IGHV4	IGKV3	8.88	C_H2	148	241
MAb M	IgG_1	κ	IGHV4	IGKV3	8.97	C_H2	152	248
MAb N	IgG_1	κ	IGHV4	IGKV3	8.85	C_H2	147	239
MAb O	IgG_1	κ	IGHV4	IGKV3	8.61	C_H2	168	274
MAb P	IgG_1	κ	IGHV4	IGKV3	8.88	C_H2	158	257
MAb Q	IgG_1	κ	IGHV4	IGKV3	9.01	C_H2	160	262
MAb R	IgG_1	κ	IGHV4	IGKV1	not tested	C_H2	129	210
MAb S	IgG_1	κ	IGHV5	IGKV1	8.88	C_H2	153	249
MAb T	IgG_1	λ	IGHV1	IGLV1	8.85	C_H2	125	203
MAb U	IgG_1	λ	IGHV3	IGLV7	8.97	C_H2	137	223
MAb V	IgG_1	λ	IGHV7	IGLV3	not tested	C_H2	108	176
MAb W	IgG_1	λ	IGHV3	IGLV1	not tested	C_H2	149	242
MAb 1	IgG_4	κ	IGHV3	IGKV3	not tested	C_H2	130	211
MAb 2	IgG_4P[d)]	κ	IGHV4	IGKV3	not tested	C_H2	129	210
MAb 3	IgG_4PE[c)]	κ	IGHV3	IGKV1	not tested	C_H2	116	188
MAb 4	IgG_4PE[c)]	κ	IGHV3	IGKV1	not tested	C_H2	117	190
MAb 5	IgG_4PE[c)]	κ	IGHV4	IGKV1	not tested	C_H2	141	229
MAb 6	IgG_4PE[c)]	κ	IGHV4	IGKV3	not tested	C_H2	124	201

[a)] Germline family was determined according to the immunogenetics nomenclature rules [31, 32].

[b)] C_{Na} can be calculated according to the following equation; $C_{Na} = 1.633 * C_{Phos} - 0.584$.

[c)] Ser228Pro and Leu235Glu mutated forms of the IgG heavy chain.

[d)] Ser228Pro mutated form of the IgG_4 heavy chain.

[e)] Presence of *N*-glycan in the V_H regions was confirmed by sugar-chain analysis.

1.3.2. Instrumentation and materials for chromatography experiment

Chromatography experiments were performed on an Alliance HPLC Workstation (Waters, Milford, MA, USA). Ceramic hydroxyapatite type II with an average bead size diameter of 20 μm (BioRad Laboratories, Hercules, CA, USA) was used as the chromatography medium and was packed into a glass column of 3-mm internal diameter and 50-mm height (Kyoshin Kogyo, Tokyo, Japan). Although type I hydroxyapatite shows high binding capacity compared to type II hydroxyapatite [33] and is widely used in industrial-scale IgG antibody applications, type II is superior in resolution to type I. Both types are also known to show similar elution characteristics. In addition, 40-μm or 80-μm bead size is commonly used for industrial-scale manufacturing to prevent high back-pressure. In the present study, we used type II hydroxyapatite of 20-μm bead size to obtain high resolution. Sodium phosphate dibasic dodecahydrate (Junsei Chemical, Tokyo, Japan), sodium phosphate monobasic dihydrate (Kokusan Chemical, Tokyo, Japan), and purified water were used to prepare chromatography buffers. All reagents used in this study were of analytical grade.

1.3.3. Hydroxyapatite chromatography

The hydroxyapatite column was equilibrated with 5 mM NaPi, pH 6.8 (buffer A). The flow rate was 0.35 mL/min. Samples were loaded onto the column at 0.035 mg rhMAb/mL hydroxyapatite. The sample injection volume was 50 μL. After washing the column with buffer A for 5 min, elution was performed for 30 min with a linear gradient, from buffer A to 400 mM NaPi, pH 6.8 (buffer B). The column was regenerated with buffer B for 2 min. To prevent strong effects of phosphate concentration on pH, the pH values of both chromatography buffers were adjusted with a calibrated pH meter by mixing 5 mM (or 400 mM) solution of sodium phosphate dibasic and the solution of sodium phosphate monobasic of the same concentration. Chromatographic runs were performed at 25°C, and the column effluent was monitored at 215 nm and 280 nm. The baseline absorbance at 215 nm increased during gradient elution, and the correlation formula between run time and phosphate concentration of the column effluent could be calculated. The peak phosphate concentration (C_{Phos}) for each rhMAb was determined according to the correlation formula and the peak retention time. The phosphate concentration and the sodium ion concentration in the prepared buffers were 4.951 mM and 7.502 mM for buffer A, and 400.0 mM and 652.8 mM for buffer B. Thus, the C_{Na} value can be calculated according to the following equation;

$$C_{Na} = 1.633 \times C_{Phos} - 0.584$$

Chromatography experiments for each rhMAb sample were conducted in duplicate, and the average of the C_{Na} values was used for interpretation. Control rhMAb (MAb A-1) was injected every 10 runs to confirm the validity of column reuse.

1.3.4. Measurement of isoelectric point

To determine isoelectric point (p*I*) values for the rhMAbs, isoelectric focusing was performed with the use of an Ampholine PAGplate (GE Healthcare) at pH 3.5−9.5. The buffer of the samples was exchanged to purified water, and 25 μg was loaded onto the gel. The running conditions were 90 min at 50 mA and 30 W. After electrophoresis, gels were stained with Coomassie brilliant blue. The p*I* value of each rhMAb was calculated with the use of the calibration curve for marker proteins included in the Broad p*I* kit (GE Healthcare). Some of the analyzed rhMAbs showed several bands in the gel. In these cases, the p*I* value of the predominant band was used.

1.3.5. Relative solvent accessibility

We searched the protein structure database RCSB Protein Data Bank (http://www.rcsb.org/pdb/) for antibodies and antibody fragments with high amino acid sequence homology to the rhMAbs used in this study. For the antibodies and antibody fragments detected, the absolute surface area of each amino acid residue was calculated with the use of the Digital Shape Sampling and Processing program [34]. The relative solvent accessibility (RSA) value for each amino acid residue was defined as the ratio of the absolute surface area of the residue observed in the three-dimensional structure to that observed in the extended tripeptide (Ala-X-Ala) conformation [35]. The extended-state absolute surface area values were the same as those reported by Ahmad et al. in Table 1.2 [35]. The RSA of each amino acid residue for the rhMAbs used in this study was estimated by calculating the mean of the RSA values of the positionally equivalent amino acid residue in the homologous antibodies and antibody fragments.

Table 1.2.
The absolute surface area values in extended tripeptide (Ala-X-Ala) conformation for each of the 20 mino acids

Amino acid residue	Absolute surface area values in extended tripeptide ($Å^2$)	Amino acid residue	Absolute surface area values in extended tripeptide ($Å^2$)
Alanine	110.2	Methionine	200.1
Aspartate	144.1	Aspartate	146.4
Cysteine	140.4	Proline	141.9
Glutamine	174.7	Glutamate	178.6
Phenylalanine	200.7	Arginine	229.0
Glycine	78.7	Serine	117.2
Histidine	181.9	Threonine	138.7
Isoleucine	185.0	Valine	153.7
Lysine	205.7	Tryptophan	240.5
Leucine	183.1	Tyrosine	213.7

1.4. Results and discussion

1.4.1. Hydroxyapatite chromatography of 37 rhMAbs

Hydroxyapatite chromatography experiments of the 37 rhMAbs by NaPi gradient elution were performed. These rhMAbs differed in their variable regions, heavy chain subclass, and light chain type (Table 1.1). Twelve rhMAbs, from MAb A-1 to MAb D-4, comprised 4 sets of variable domain-identical antibodies. The MAbs of each set differed only in subclass (IgG_1, IgG_2, IgG_4, or IgG_4PE). Amino acid sequences of the variable regions of the 23 IgG_1, 4 IgG_2, and 10 IgG_4 (including 1 IgG_4P and 6 IgG_4PE) rhMAbs showed sufficient variety for the present study. This is also shown in Table 1.1 as variety of the germline families of the V_H and V_L regions.

The C_{Na} and C_{Phos} values of individual rhMAbs are also shown in Table 1.1. The calculated standard deviation of the C_{Na} values for the control rhMAbs was 1.8 mM, and the coefficient of variation was 0.6%, indicating the high reproducibility of this method.

1.4.2. Relation between antibody structure and retention time

The obtained C_{Na} values are compared in Fig. 1.1. An elution order according to subclass (IgG_2 < IgG_4, IgG_4PE < IgG_1) was observed for each of the 4 sets of variable domain-identical rhMAbs (MAbs A-1 to D-4). The observed elution order for subclass isotypes was different from that in cation-exchange chromatography, where elution behavior does not depend on subclass [17]. The elution order in hydroxyapatite chromatography was observed even for rhMAbs containing an *N*-glycan in each of the V_H regions (MAbs D-1, D-2, and D-4). Similarly, point mutations in the IgG_4 rhMAbs did not change the elution order. In addition, the λ IgG_1 rhMAbs (MAbs T to W; average C_{Na} being 211 mM) tended to elute earlier than the κ IgG_1 rhMAbs (average C_{Na} being 257 mM). In relation to the variable regions, variation in the C_{Na} values was also observed among the subclass-identical rhMAbs with the same light chain type. From these results, we concluded that all aspects of subclass, light chain type, and variation of amino acid sequence in the variable regions must be taken into account to classify the C_{Na} values of human IgG MAbs in the NaPi gradient hydroxyapatite chromatography. Interestingly, MAb D-1, containing an *N*-glycan in each of the V_H regions, showed the smallest C_{Na} value among all of the κ IgG_1 rhMAbs, suggesting that the presence of *N*-glycan in the V_H regions also affects the retention behavior.

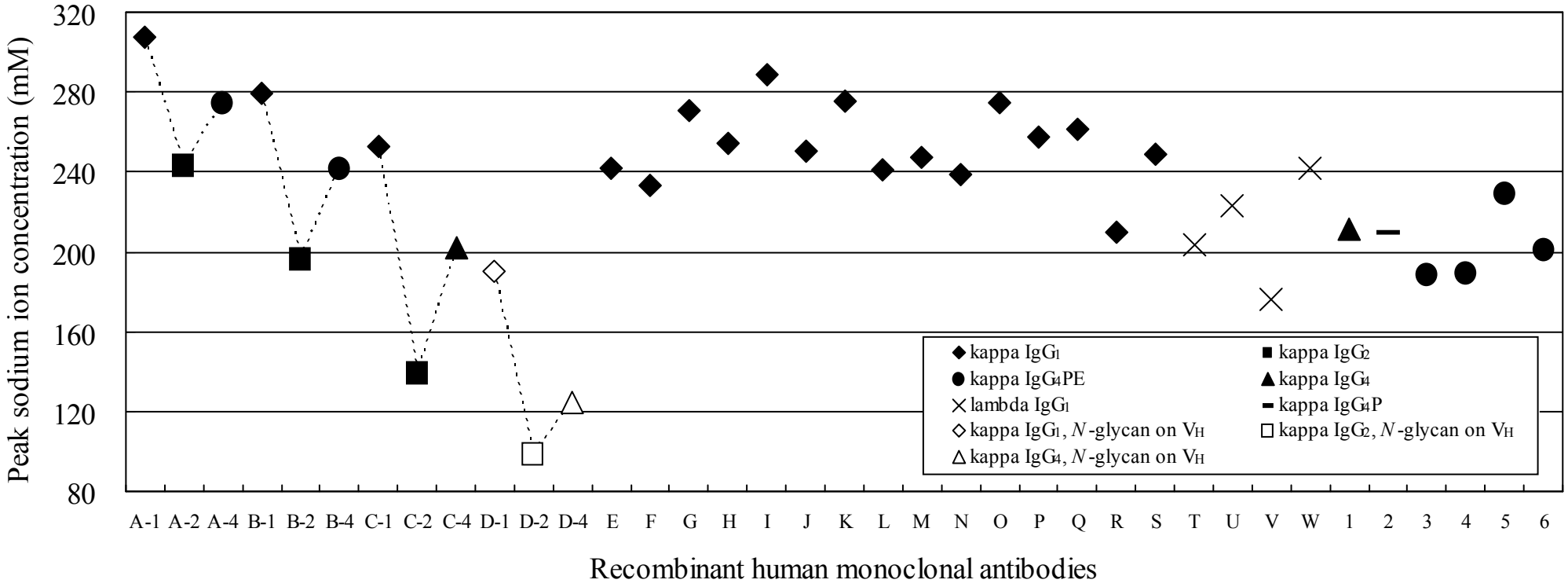

Fig. 1.1. Peak sodium ion concentration values of rhMAbs in hydroxyapatite chromatography.

1.4.3. Relation between acidic and basic amino acid residues and retention time

The C_{Na} or C_{Phos} values for 34 rhMAbs (excluding MAbs D-1 to D-4) were compared according to the number of the following acidic and basic amino acid residues in the entire antibody: arginine (Arg), lysine (Lys), histidine (His), glutamate (Glu), and aspartate (Asp). Figure 1.2 shows a relatively higher correlation between C_{Na} and the number of basic residues (correlation coefficient: $r^2 = 0.50$ for Arg, Lys, and His; Fig. 1.2A) than between C_{Phos} and the number of acidic residues ($r^2 = 0.00$ for Glu and Asp; Fig. 1.2B) or between C_{Na} and the number of acidic and basic residues ($r^2 = 0.24$ for Arg, Lys, His, Glu, and Asp; Fig. 1.2C). This result suggested that the number of basic residues is correlated with retention behavior.

(A)

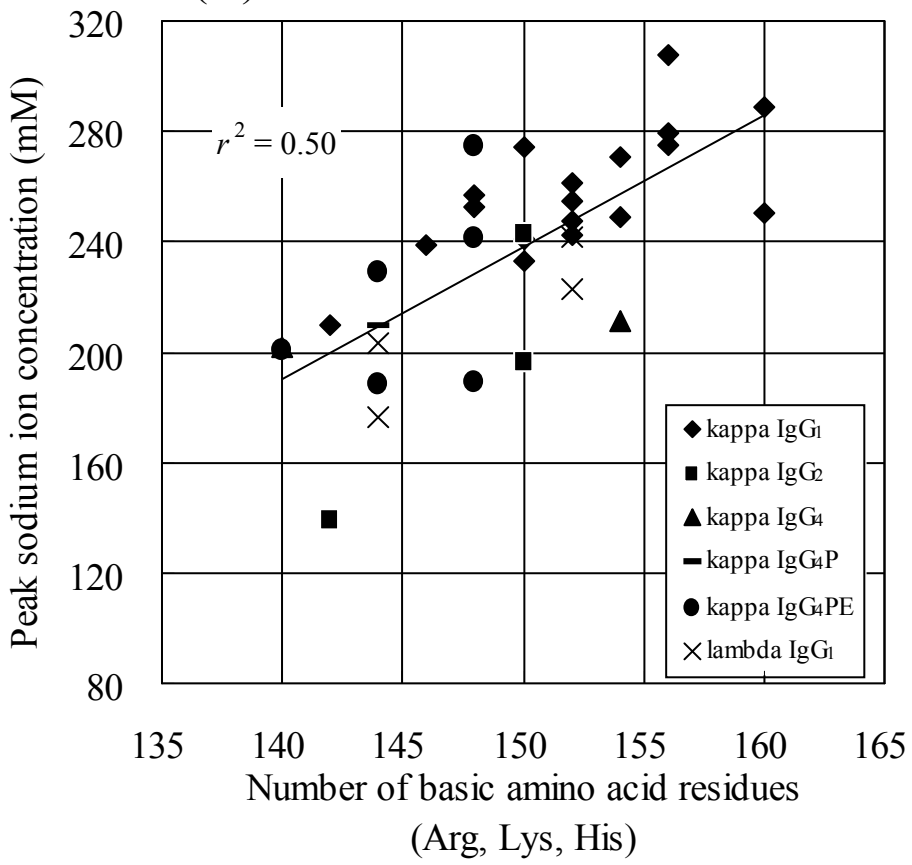
Peak sodium ion concentration (mM)
320
280
240
200
160
120
80
$r^2 = 0.50$
kappa IgG1
kappa IgG2
kappa IgG4
kappa IgG4P
kappa IgG4PE
lambda IgG1
135
140
145
150
155
160
165
Number of basic amino acid residues
(Arg, Lys, His)

(B)

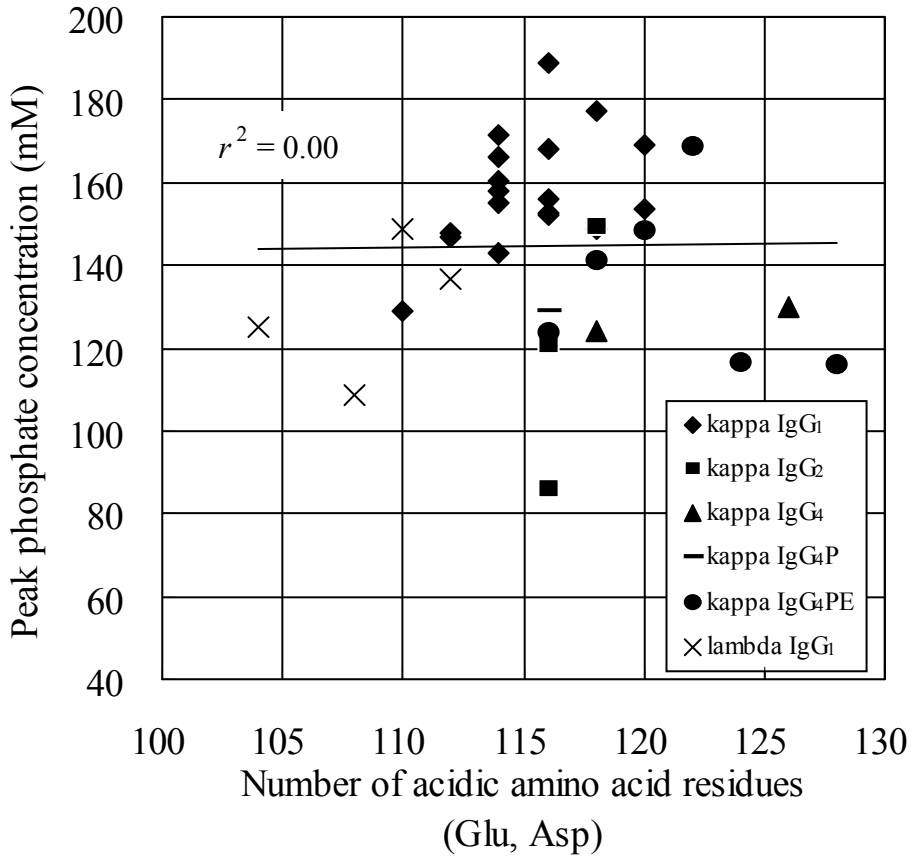
Peak phosphate concentration (mM)
200
180
160
140
120
100
80
60
40
$r^2 = 0.00$
kappa IgG1
kappa IgG2
kappa IgG4
kappa IgG4P
kappa IgG4PE
lambda IgG1
100
105
110
115
120
125
130
Number of acidic amino acid residues
(Glu, Asp)

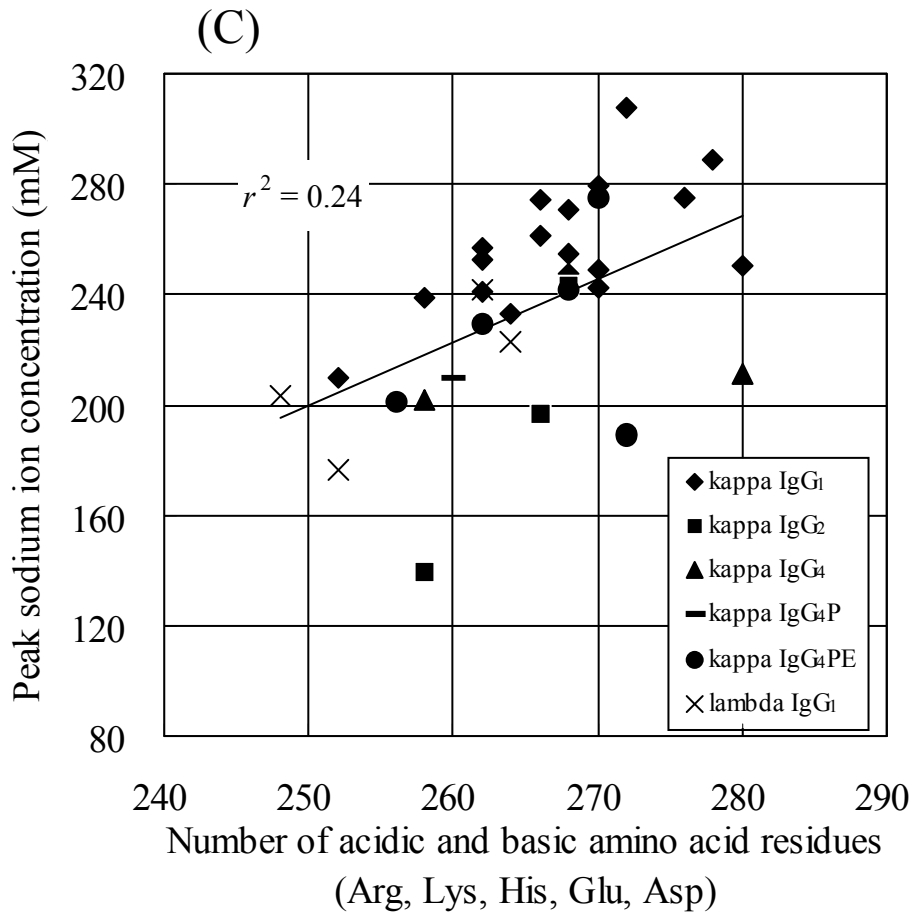

Fig. 1.2. Relation between the numbers of acidic and basic amino acid residues in the entire antibody molecule and peak sodium ion or phosphate concentration in hydroxyapatite chromatography for 34 rhMAbs(excluding MAbs D-1, D-2, and D-4). (A) Basic amino acid residues (Arg, Lys, and His); (B) acidic amino acid residues (Glu and Asp); (C) acidic and basic amino acid residues (Arg, Lys, His, Glu, and Asp). Correlation coefficient in each panel was calculated using the values for all 34 rhMAbs.

The relation between p*I* and C_{Na} was investigated for the 25 rhMAbs (MAbs A-1 to C-4, E to Q, and S to U) (Fig. 1.3). The p*I* value provides a simple indication of the net charge of proteins, and the chromatographic behavior of proteins is usually explained by their p*I* values and the mobile-phase pH in ion-exchange chromatography. The result of the present study showed a weak correlation ($r^2 = 0.43$). No significant correlations were found, however, among members of each antibody group (κ IgG_1, κ IgG_2, etc.). Thus, it was indicated that the retention behavior of rhMAbs in hydroxyapatite chromatography cannot be determined simply by net charge properties.

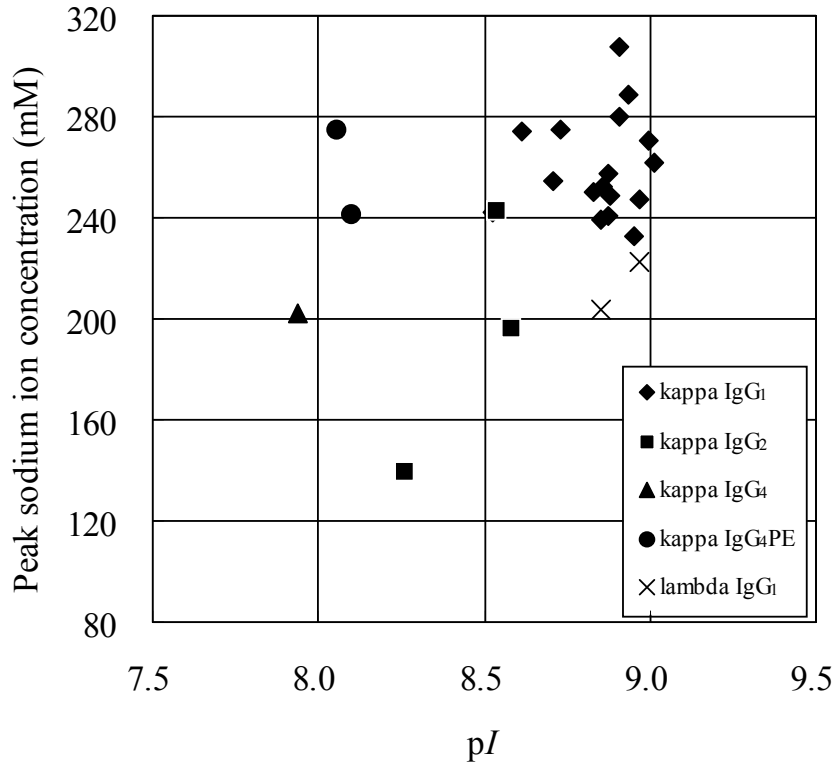

Fig. 1.3. Plots of isoelectric point (p*I*) values versus peak sodium ion concentration values for the 25 rhMAbs. p*I* values were determined by isoelectric focusing.

Although the metal-affinity interaction between carboxyl clusters of acidic residues on proteins and C-sites has been suggested to be involved in antibody adsorption, the number of acidic residues did not show a correlation with C_{Phos} (Fig. 1.2B). In most cases, a low concentration of phosphate ion (ca. 5–15 mM) is necessary for the elution of IgG antibodies in hydroxyapatite chromatography with NaCl gradient elution [33]. However, the C_{Phos} value of antibodies with NaPi gradient elution (ca. 60–190 mM in the present study, Table 1.1) was much higher than that required for NaCl gradient elution. These results suggested that the metal-affinity interaction is already eliminated before the dissociation of cation exchange interactions between positively charged amino acid residues and P-sites [4, 33]. The involvement of the metal-affinity interactions in the adsorption of rhMAbs onto hydroxyapatite is described in CHAPTER 2.

Next, antibody structure (subclass, light chain type, and V_H or V_L regions) was taken into consideration in an attempt to identify relevant parameters to correlate better with C_{Na}. Table 1.3 shows the r^2 values calculated between C_{Na} and various combinations of the number of acidic and basic residues in one or both of the V_H and V_L regions of the 18 κ IgG_1 rhMAbs (excluding MAb D-1). The results indicated that the number of basic residues (Arg, Lys, and His) in the V_H regions showed a stronger correlation ($r^2 = 0.55$) with C_{Na} than the number of basic residues in the V_L regions ($r^2 = 0.00$) or the number of

basic residues in both the V_H and V_L regions (r^2 = 0.46). This tendency was also observed for the 4 λ IgG_1 rhMAbs, the 3 κ IgG_2 rhMAbs, and the 9 κ IgG_4 rhMAbs, including IgG_4P and IgG_4PE rhMAbs (data not shown). From these results, we concluded that the retention behavior of subclass-identical rhMAbs with same type of light chains in NaPi gradient hydroxyapatite chromatography depended on the properties of the basic amino acid residues in the V_H regions more than those in the V_L regions.

Table 1.3.
Correlation coefficient (r^2) between the number of acidic and basic residues in one or both of the V_H and V_L regions and peak sodium ion concentration for the 18 κ IgG_1 rhMAbs

	Arg	Lys	His	Glu	Asp	Basic amino acid residue (Arg, Lys, His)	Acidic and basic residues (Arg, Lys, His, Glu, Asp)
V_H	0.26	0.05	0.21	0.08	0.03	0.55	0.39
V_L	0.00	0.00	0.00	0.05	0.00	0.00	0.03
$V_H + V_L$	0.27	0.04	0.13	0.14	0.01	0.46	0.40

1.4.4. Contribution of variable region to retention time

To obtain a more relevant correlation between the number of basic amino acid residues and C_{Na}, the surface accessibility of each basic residue was taken into account. The solvent-accessible surface area of each amino acid residue in a protein can be computed with bioinformatics software when three-dimensional structural information of the protein can be obtained [34]. The surface accessibility of the side chain of each amino acid residue is represented as the RSA percentage by calculating the ratio of the absolute surface area of the residue of the three-dimensional structure to that observed in the extended tripeptide (Ala-X-Ala) conformation [35].

Each of the V_H and V_L regions of human IgG is known to share structural similarity [25]. Although the three-dimensional structures of the rhMAbs used in the present study have not yet been determined, they can be estimated reliably by homology modeling of the structures of antibodies and antibody fragments with similar amino acid sequences. In the present study, the side chain RSA values of each basic residue in the variable regions for all of the rhMAbs were estimated, and the correlation between the number of basic residues with various surface accessibility cut-off values and C_{Na} was investigated.

For the 18 κ IgG_1 rhMAbs (MAbs A-1, B-1, C-1, and E to S), the plot of C_{Na} against the number of basic residues with > 40% RSA in the V_H regions (r^2 = 0.87; Fig. 1.4B)

showed a higher correlation coefficient compared to that in the plot that did not take surface accessibility of each basic residue into account (r^2 = 0.55; Fig. 1.4A). Similarly, with respect to the 4 λ IgG_1 rhMAbs (MAbs T to W), the correlation was also improved (from r^2 = 0.94 to r^2 = 0.99; Figs. 1.4A, B) when surface accessibility was considered. This tendency was also observed for the IgG_2 rhMAbs (r^2 improved from 0.95 to 1.00) and the IgG_4 rhMAbs (including IgG_4P and IgG_4PE mutated forms; r^2 improved from 0.25 to 0.80). These results indicated that the retention behavior of subclass-identical rhMAbs consisting of same type of light chains showed a clear correlation with the number of surface-exposed basic amino acid residues in the V_H regions in hydroxyapatite chromatography with NaPi gradient elution. It was thus considered that the main interaction mechanism between rhMAbs and hydroxyapatite, which contributed to the retention behavior, was cation exchange.

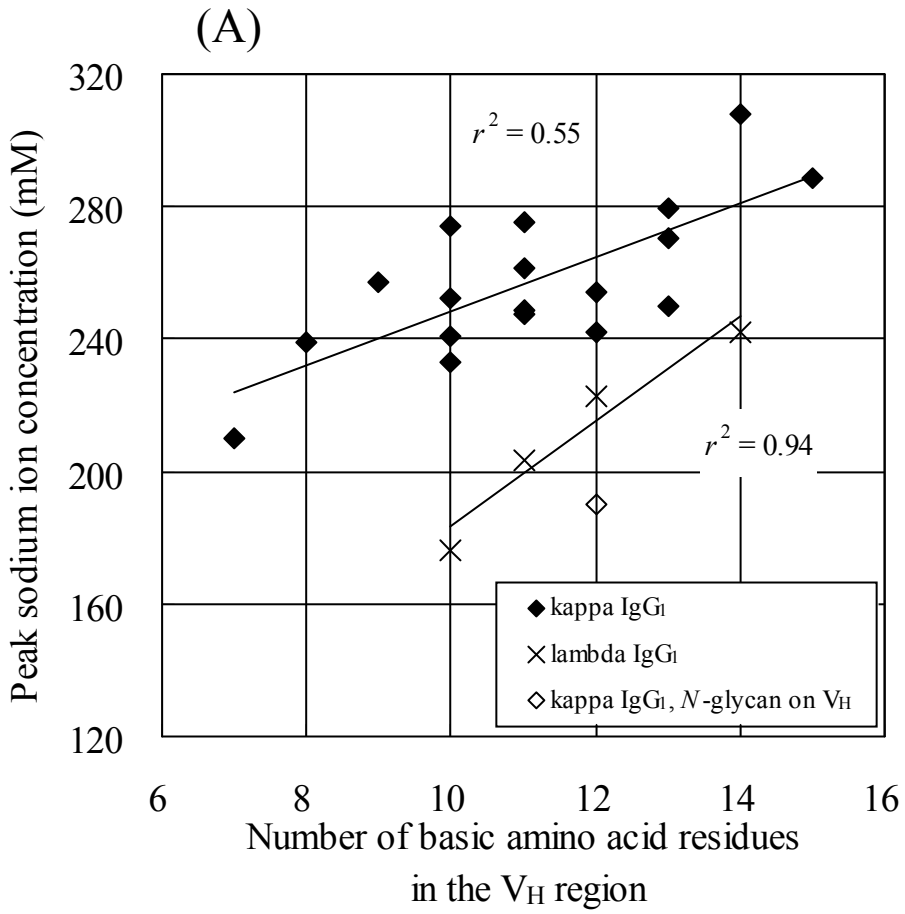
(A)
320
280
240
200
160
120
Peak sodium ion concentration (mM)
$r^2 = 0.55$
$r^2 = 0.94$
kappa IgG1
lambda IgG1
kappa IgG1, N-glycan on VH
6
8
10
12
14
16
Number of basic amino acid residues
in the VH region

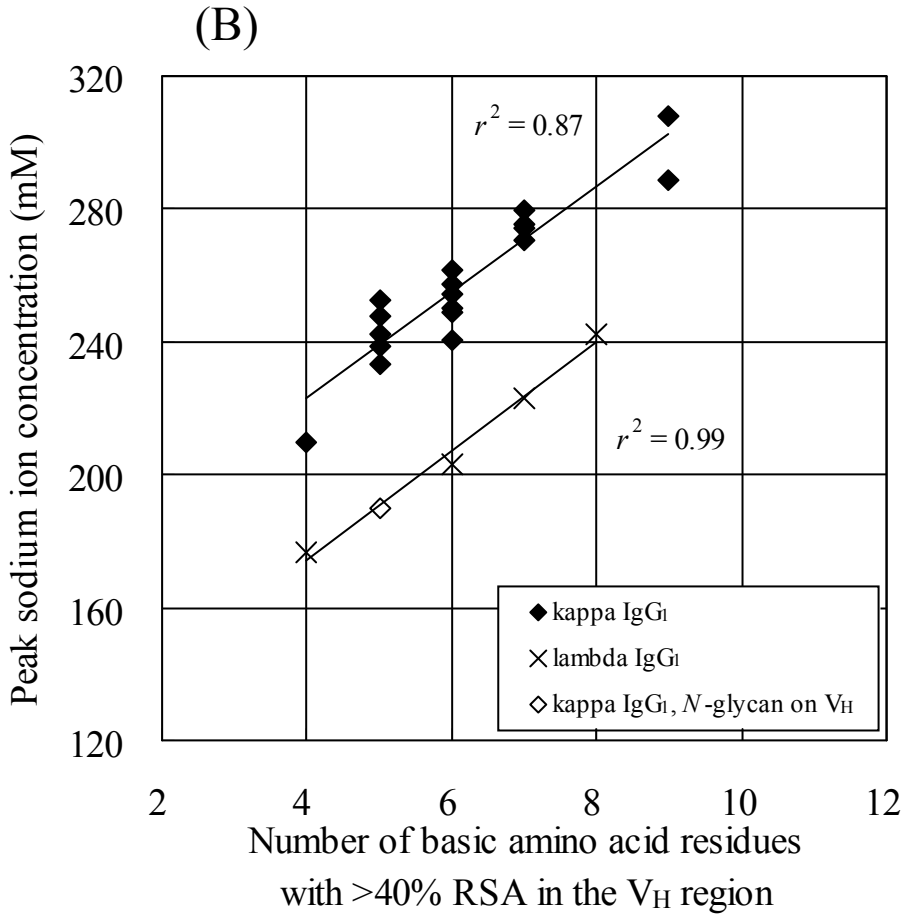
(B)
320
280
240
200
160
120
Peak sodium ion concentration (mM)
$r^2 = 0.87$
$r^2 = 0.99$
kappa IgG1
lambda IgG1
kappa IgG1, N-glycan on VH
2
4
6
8
10
12
Number of basic amino acid residues
with >40% RSA in the VH region

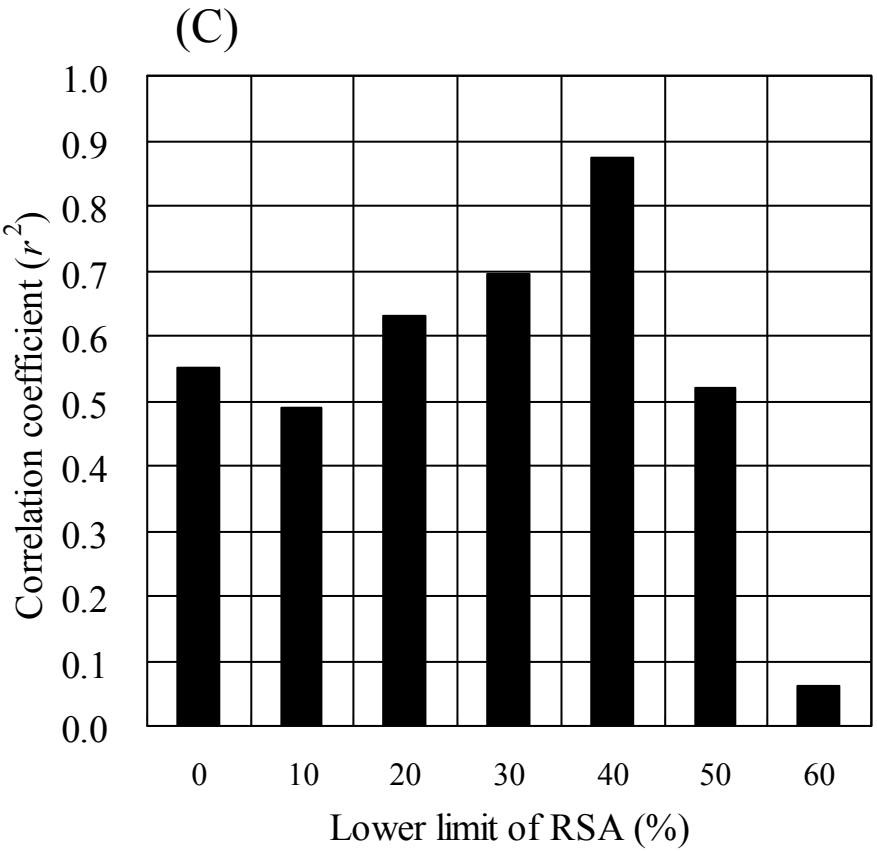

Fig. 1.4. Comparison between the number of basic amino acid residues (Arg, Lys, and His) in the V_H regions and the peak sodium ion concentration for the 18 κ IgG_1 rhMAbs (MAbs A-1, B-1, C-1, and E–S), 1 κ IgG_1 rhMAb containing an *N*-glycan in each of the V_H regions (MAb D-1), and 4 λ IgG_1 rhMAbs (MAbs T–W). Numbers of basic amino acid residues were counted on one side of the 2 variable domains. Peak sodium ion concentration versus the number of (A) basic amino acid residues and (B) basic amino acid residues with > 40% relative solvent accessibility (RSA). (C) Correlation coefficients between peak sodium ion concentration and the number of high surface-accessible basic amino acid residues in the V_H regions, with various lower limits of RSA (0%–60%) for the 18 κ IgG_1 rhMAbs.

Figure 1.4C shows the correlation coefficients between C_{Na} and the number of basic amino acid residues in the V_H regions, with different lower limits of RSA for the 18 κ IgG_1 rhMAbs. The results indicated that the basic residues on the protein surface are involved in the interaction with hydroxyapatite; the number of basic residues with > 40% RSA showed the highest correlation coefficient.

We mentioned that the number of basic residues in the V_H regions showed a stronger correlation with C_{Na} than the ones in the V_L or the whole (V_H and V_L) regions (Table 1.3). To investigate the differential contribution of the two regions to the elution behavior, we examined the correlation between the number of basic residues with > 40% RSA in whole (V_H and V_L) regions and C_{Na} for the 18 κ IgG_1 rhMAbs. The calculated correlation coefficient (r^2 = 0.68; not shown) was again smaller than that for the V_H regions only r^2 = 0.87; Fig. 1.4B). The differential contribution from the V_H and V_L regions may be due to some differential structural geometry of binding surfaces of the two regions.

The correlation was slightly higher when the number of His residues was included in the calculation of the r^2 value (for the 18 κ IgG_1 rhMAbs, r^2 = 0.55 vs. 0.53 in Fig. 1.4A; r^2 = 0.87 vs. 0.81 in Fig. 1.4B). Histidine has a weak basic imidazole group in the side chain, and the pK_a value of the imidazole group is 5.97. Thus, the imidazole side chains are expected to be positively charged partially (13%, according to the

Henderson–Hasselbalch equation) in the buffer conditions used in the present study (pH 6.8). The better correlation when the His residues were taken into account may be ascribed to this partial positive charges on the side chains of His. Although His residues may also be involved in the adsorption to C-sites on hydroxyapatite via the metal affinity interaction [12], it is unlikely, however, that such a metal-affinity interaction between His residues and C-sites would be sustained at the high concentration of displacer phosphate ion at elution. Whatever the reason, it may be appropriate to take the number of the surface-distributed His residues into account in interpreting the retention behavior of rhMAbs in NaPi gradient hydroxyapatite chromatography.

1.4.5. Contribution of constant region to retention time

Figures 1.4A and 1.4B showed that the λ IgG_1 rhMAbs (MAbs T to W) did not follow the correlation curve of the κ IgG_1 rhMAbs, despite the sufficient structural similarity of the λ and κ framework regions [25]. Because the number of basic amino acid residues was counted only in the V_H region, this differential retention behavior was thought to be caused by differences in the number of basic residues in the light chain constant (C_L) region between λ and κ IgG_1 rhMAbs. However, the number of basic amino acid residues with > 40% RSA in the λ and κ C_L regions (λ C_L being IGLC1, IGLC2, and IGLC3 according to the IMGT nomenclature rules) was the same (seven). With respect to the difference of λ and κ antibodies, it is known that λ chains exhibit much wider range of the elbow angle (the angle between the variable and constant domains of light chain) than κ chains, and the flexibility of the light chain is thought to affect ligand binding [36, 37]. Such a difference in conformational flexibility between λ and κ antibodies may influence the accessibility of the binding sites to hydroxyapatite.

In Fig. 1.5, the number of basic residues with > 40% RSA in the V_H region is plotted against C_{Na} for the 37 rhMAbs. When these 37 rhMAbs were classified according to their subclass and type of light chain, each group showed a linear correlation with a similar slope. Therefore, the C_{Na} values of rhMAbs on hydroxyapatite with NaPi gradient

elution can be classified by the type of constant regions (subclass, type of light chains) and the number of surface-distributed basic amino acid residues in the V_H regions. In relation to IgG_4 rhMAb and IgG_4 mutated forms (IgG_4P and IgG_4PE), the correlation curve showed a high correlation coefficient value ($r^2 = 0.80$). Although the Ser228Pro and Leu235Glu point mutations are known to be effective in preventing half-antibody formation and in reducing antibody-dependent cytotoxicity [29, 30], these mutations did not influence the retention behavior.

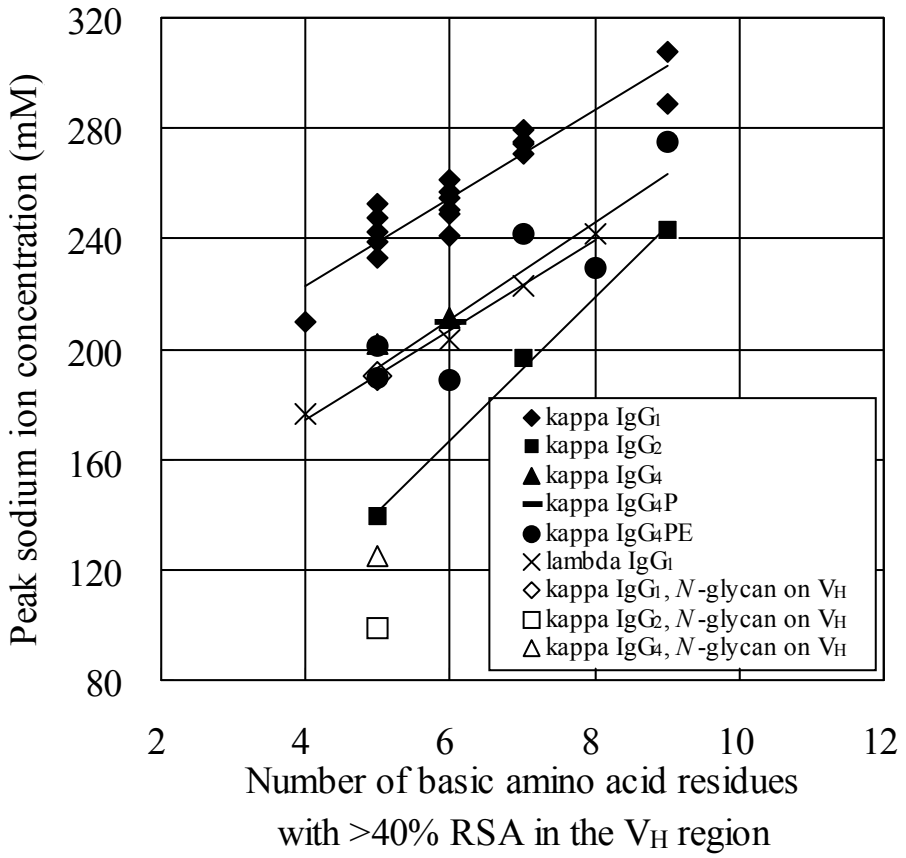

Fig. 1.5. Comparison between the number of basic amino acid residues (Arg, Lys, and His) with > 40% RSA in the V_H region and peak sodium ion concentration for the 37 rhMAbs. Correlation curves, from the top, were calculated for the 18 kappa IgG_1 rhMAbs, 9 IgG_4 rhMAbs (including IgG_4P and IgG_4PE rhMAbs), 4 lambda IgG_1 rhMAbs, and 3 IgG_2 rhMAbs. The rhMAbs containing an *N*-glycan in each of the V_H regions (MAbs D-1, D-2, and D-4) were not included in the calculation of the correlation curves.

In clear contrast to results of cation-exchange chromatography with rhMAbs [17], the retention behavior with NaPi gradient hydroxyapatite chromatography was affected by antibody subclass. The reasons for the differential interaction according to subclass may include the differential distribution of basic amino acid residues on the heavy chain constant regions, which will become clear when three-dimensional structural information for IgG_2 and IgG_4 antibodies becomes available.

1.4.6. Effect of *N*-glycan linked to V_H region on retention time

The MAb D-1, which is classified as κ IgG_1 and contains an *N*-glycan in each of the V_H regions, eluted the earliest among the 19 κ IgG_1 rhMAbs (Fig. 1.1). In addition, MAb D-1 showed a clear deviation from the correlation curve of the 18 κ IgG_1 rhMAbs without *N*-glycan, (Fig. 1.4B). This deviation of rhMAbs with *N*-glycan in their V_H regions from the correlation curves of their subclass-identical rhMAbs was also observed for MAbs D-2 and D-4 (Fig. 1.5). According to amino acid sequence analysis and structural homology modeling, the glycosylation sites of MAbs D-1, D-2, and D-4 are estimated to be located at the tips of the V_H regions, which are between the second and third complementarity-determining regions. This suggests that the presence of *N*-glycan in the V_H regions inhibits the interaction of this region with hydroxyapatite. In addition,

Kishino et al. reported that various glycoforms of human serum alpha1-acid glycoprotein can be separated by phosphate gradient hydroxyapatite chromatography and that glycoforms with highly branched glycan chains tended to elute earlier than those with poorly branched glycan chains [38]. Furthermore, Melcher et al. reported that among mutants of human lysozyme, the one with the highest carbohydrate content eluted first from hydroxyapatite [39]. These reports are in agreement with our present observations and suggest that *N*-glycan in the V_H regions of MAbs D-1, D-2, and D-4 interferes with binding to hydroxyapatite.

1.5. Concluding remarks

A survey of hydroxyapatite retention of 37 structurally well-characterized IgG rhMAbs using NaPi gradient elution revealed that the retention time (C_{Na}) can be classified according to the subclass (IgG_1 > IgG_4 > IgG_2), type of light chain (κ IgG > λ IgG), and the number of surface-distributed basic amino acid residues in the V_H regions (positive linear relation with C_{Na}). Though it was therefore supposed that the main retention mechanism of rhMAbs on hydroxyapatite was cation exchange interaction, the result that subclass affected the retention behavior was different from a simple cation-exchange chromatography. These findings should be helpful to investigators and purification-process developers working with antibodies.

1.6. References

[1] Tiselius, A., Hjertén, S., Levin, Ö., Arch. *Biochem. Biophys.* 1956, *65*, 132-155.

[2] Gagnon, P., *Purification Tools for Monoclonal Antibodies*, Validated Biosystems, San Clemente, U.S.A. 1996, pp. 87-102.

[3] Horenstein, A. L., Crivellin, F., Funaro, A., Said, M., Malavasi, F., *J. Immunol. Methods* 2003, *275*, 99-112.

[4] Gagnon, P., Ng, P., Zhen, J., Aberin, C., He, J., Mekosh, H., Cummings, L., Zaidi, S., Richieri, R., *Bioprocess Int.* 2006, *4*, 50-60.

[5] Roque, A. C. A., Silva, C. S. O., Taipa, M. A., *J. Chromatogr. A* 2007, *1160*, 44-55.

[6] Wensel, D. L., Kelley, B. D., Coffman, J. L., *Biotechnol. Bioeng.* 2008, *100*, 839-854.

[7] Gagnon, P., *N. Biotechnol.* 2009, *25*, 287-293.

[8] Bernardi, G., *Methods Enzymol.* 1973, *27*, 471-479.

[9] Gorbunoff, M. J., *Anal. Biochem.* 1984, *136*, 425-432.

[10] Gorbunoff, M. J., *Anal. Biochem.* 1984, *136*, 433-439.

[11] Gorbunoff, M. J., Timasheff, S. N., *Anal. Biochem.* 1984, *136*, 440-445.

[12] Ng, P. K., He, J., Gagnon, P., *J. Chromatogr. A* 2007, *1142*, 13-18.

[13] Juarez-Salinas, H., Ott, G. S., Chen, J. C., Brooks, T. L., Stanker, L. H., *Methods Enzymol.* 1986, *121*, 615-622.

[14] Vola, R., Lombardi, A., Mariani, M., *BioTechniques* 1993, *14*, 650-655.

[15] Schubert, S., Freitag, R., *J. Chromatogr. A* 2009, *1216*, 3831-3840.

[16] Gagnon, P., Cheung, C., Yazaki, P. J., *J. Immunol. Methods* 2009, *342*, 115-118.

[17] Ishihara, T., Kadoya, T., Yoshida, H., Tamada, T., Yamamoto, S., *J. Chromatogr. A* 2005, *1093*, 126-138.

[18] Shukla, A. A., Hubbard, B., Tressel, T., Guhan, S., Low, D., *J. Chromatogr. B* 2007, *848*, 28-39.

[19] Coffman, J. L., Kramarczyk, J. F., Kelley, B. D., *Biotechnol. Bioeng.* 2008, *100*, 605-618.

[20] Ghose, S., Allen, M., Hubbard, B., Brooks, C., Cramer, S. M., *Biotechnol. Bioeng.* 2005, *92*, 665-673.

[21] Ladiwala, A., Rege, K., Breneman, C. M., Cramer, S. M., *Proc. Natl. Acad. Sci. U.S.A.* 2005, *102*, 11710-11715.

[22] Lienqueo, M. E., Salazar, O., Henriquez, K., Calado, C. R. C., Fonseca, L. P., Cabral, J. M. S., *J. Chromatogr. A* 2007, *1154*, 460-463.

[23] Kramarczyk, J. F., Kelley, B. D., Coffman, J. L., *Biotechnol. Bioeng.* 2008, *100*, 707-720.

[24] Burton, D. R., Gregory, L., Jefferis, R., *Monogr. Allergy* 1986, *19*, 7-35.

[25] Honegger, A., Plückthun, A., *J. Mol. Biol.* 2001, *309*, 657-670.

[26] Ishida, I., Tomizuka, K., Yoshida, H., Tahara, T., Takahashi, N., Ohguma, A., Tanaka, S., Umehashi, M., Maeda, H., Nozaki, C., Halk, E., Lonberg, N., *Cloning Stem Cells* 2002, *4*, 91-102.

[27] Salfeld, J. G., *Nat. Biotechnol.* 2007, *25*, 1369-1372.

[28] Kabat, E. A., Wu, T. T., Perry, H. M., Gottesman, K. S., Foeller, C., *Sequences of Proteins of Immunological Interest (5th ed.)*, Public Health Service, National Institutes of Health, Bethesda, U.S.A. 1991.

[29] Angal, S., King, D. J., Bodmer, M. W., Turner, A., Lawson, A. D. G., Roberts, G., Pedley, B., Adair, J. R., *Mol. Immunol.* 1993, *30*, 105-108.

[30] Reddy, M. P., Kinney, C. A. S., Chaikin, M. A., Payne, A., Fishman-Lobell, J., Tsui, P., Monte, P. R. D., Doyle, M. L., Brigham-Burke, M. R., Anderson, D., Reff, M., Newman, R., Hanna, N., Sweet, R. W., Truneh, A., *J. Immunol.* 2000, *164*, 1925-1933.

[31] WHO-IUIS *Nomenclature SubCommittee for Immunoglobulins and T cell receptors report*, 13th International Congress of Immunology, Rio de Jaeiro, Brazil 2007.

[32] Lefranc, M. P., Pommié, C., Kaas, Q., Duprat, E., Bosc, N., Guiraudou, D., Jean, C., Ruiz, M., Piédade, I. D., Rouard, M., Foulquier, E., Thouvenin, V., Lefranc, G., *Dev.*

Comp. Immunol. 2005, *29*, 185-203.

[33] Gagnon, P., Ng, P., He, J., Zhen, J., Aberin, C., Mekosh, H., *232th ACS National Meeting*, Aneheim, U.S.A. 2006.

[34] Kabsch, W., Sander, C., *Biopolymers* 1983, *22*, 2577-2637.

[35] Ahmad, S., Gromiha, M., Fawareh, H., Sarai, A., *BMC Bioinformatics* 2004, *5*, 51-55.

[36] Huber, R., Deisenhofer, J., Colman, P. M., Matsushima, M., Palm, W., *Nature* 1976, *264*, 415-420.

[37] Stanfield, R. L., Zemla, A., Wilson, I. A., Rupp, B., *J. Mol. Biol.* 2006, *357*, 1566-1574.

[38] Kishino, S., Nomura, A., Saitoh, M., Sugawara, M., Iseki, K., Kitabatake, A., Miyazaki, K., *J. Chromatogr. B* 1997, *703*, 1-6.

[39] Melcher, R., Hillebrand, A., Bahr, U., Schroder, B., Karas, M., Hasilik, A., *Biochem. J.* 2000, *348*, 507-515.

CHAPTER 2

Relationship between human IgG structure and retention time in hydroxyapatite chromatography with sodium-chloride gradient elution

2.1. Summary

Accurate prediction of the elution tendency of monoclonal antibodies in column chromatography would be beneficial for the efficient setup of purification procedures. Hydroxyapatite chromatography experiments using 37 recombinant human monoclonal antibodies were performed by sodium-chloride gradient elution with 5 mM sodium phosphate to correlate the retention times with antibody structures (subclass and light chain isotypes). The contribution of metal affinity interactions in the interaction of antibodies with hydroxyapatite was investigated by (1) eliminating 5 mM sodium phosphate in buffers, (2) comparing sodium-chloride vs. sodium-phosphate gradient elutions, and (3) using IgG_4 antibodies with a leucine $\rightarrow$ glutamate mutation. By using antibodies of different subclasses but with identical Fab regions, the elution behavior in sodium-chloride elution could be classified by subclass and type of light chain. It is considered that the retention of monoclonal antibodies to hydroxyapatite is affected by the cooperation of phosphoryl cation exchange and metal affinity interactions. The contribution of the metal affinity interactions is greater in the sodium-chloride gradient elution method than in the sodium-phosphate gradient elution method.

2.2. Introduction

Hydroxyapatite chromatography [1] has been applied as an efficient tool for the purification of recombinant monoclonal antibodies (rMAbs) because it offers high selectivity and can be performed under neutral pH conditions [2–5]. Two fundamentally different interaction mechanisms are mainly involved in hydroxyapatite chromatography of proteins [6–9]: (1) a phosphoryl cation exchange interaction between positively charged amino acid residues on proteins and phosphate functional groups of hydroxyapatite (P-sites), and (2) a calcium-metal-affinity interaction between carboxyl clusters on proteins and calcium functional groups of hydroxyapatite (C-sites). This complexity of the interaction mechanisms makes it difficult to predict or classify retention behavior.

Diverse studies have been conducted on the interaction of rMAbs and hydroxyapatite. By a high-throughput screening system using 96-well plates dispensed with hydroxyapatite resin, Wensel et al. examined the binding of 15 humanized MAbs under various combinations of sodium phosphate (NaPi), sodium chloride (NaCl), and pH [10]. They showed that there was a wide variation in MAb binding strengths to hydroxyapatite, and that the logarithm of the partition coefficients of MAbs to hydroxyapatite is linearly correlated with pH, log[sodium chloride], and log[total phosphate]. In addition, there

were no consistent trends in binding with regard to antibody characterization parameters (e.g., light chain isotype, CDR classification), except that IgG_2 MAbs showed least overall binding. Schubert and Freitag used a recombinant human κ IgG_1 antibody and electrostatic modeling techniques to demonstrate that electrostatic interactions via Fab (fragment, antigen binding) regions play an important role in the absorption to hydroxyapatite [11]. Furthermore, Gagnon et al. showed that papain-digested Fab regions of a chimeric MAb failed to bind to calcium-derivatized hydroxyapatite [12]. On the other hand, in our previous study, we examined the retention behavior of recombinant human MAbs (rhMAbs), which included antibodies of different subclasses but with identical Fab regions, in hydroxyapatite chromatography by the NaPi gradient method. We showed that the retention time can be classified by subclass (IgG_2 < IgG_4 < IgG_1), type of light chain (λ IgG < κ IgG), and the number of surface distributed basic amino acid residues (arginine, lysine, and histidine) in the heavy chain variable regions (V_H regions) [13].

In this study, we examined the retention times (peak NaCl concentration values (C_{NaCl})) of 37 rhMAbs to correlate the retention behavior of rhMAbs with the antibody structures in hydroxyapatite chromatography by NaCl gradient elution. The C_{NaCl} values obtained were compared with the retention times by NaPi gradient elution to improve

our understanding of the interaction mechanisms between rhMAbs and hydroxyapatite.

2.3. Experimental

2.3.1. Recombinant human monoclonal antibodies

All rhMAbs used in this study were identical to those used in our previous study of NaPi gradient elution experiments [13]. They were produced in suspension cultures of Chinese hamster ovary cells, which were transfected with vectors containing antibody genes cloned from human antibody-producing mice [14]. Protein A affinity chromatography purification of cell culture supernatants was performed by low pH stepwise elution using MabSelect or Protein A Sepharose FF columns (GE Healthcare, Buckinghamshire, UK). Further purification steps (cation-exchange, anion-exchange in flow-though mode, and/or hydrophobic chromatography) were performed as necessary to improve protein purity. The purified rhMAbs were buffer-exchanged to 5 mM NaPi (pH 6.8) with the use of Amicon Ultra-4 10K molecular-weight cutoff centrifugal filter units (Millipore, Billerica, MA, USA), and the antibody concentration was adjusted to 250 μg/mL.

The classification of the 37 rhMAbs according to their physicochemical properties is shown in Table 2.1. IgG_3 rhMAb was not used because IgG_3 antibody is difficult to handle for manufacturing and therapeutic purposes due to its low binding capacity on the protein A adsorbent and to its high sensitivity to proteolysis [15, 16]. The 10 IgG_4

rhMAbs (MAbs A-4, B-4, C-4, D-4, and 1 to 6) were also classified according to inserted point mutations: three wild-type IgG_4 MAbs, one IgG_4P mutated MAb, and six IgG_4PE mutated MAbs. The IgG_4P MAb contains an amino acid point mutation of Ser228Pro in the heavy chain of IgG_4 (EU-index numbering scheme [17] used throughout) to prevent half-antibody formation [18]. The IgG_4PE MAbs additionally contain a Leu235Glu point mutation in the heavy chain to reduce antibody-dependent cellular cytotoxicity [19]. Twelve rhMAbs from MAb A-1 to MAb D-4 comprise four sets of three subclass isotypes. Thus, the amino acid sequences of the light chains and V_H regions in each set are identical, but their subclasses are different (IgG_1, IgG_2, IgG_4, or IgG_4PE). MAbs D-1, D-2, and D-4 contain an *N*-glycan structure in each of the V_H regions. The glycosylation site is estimated to be located on the tips of the V_H regions between the second and third complementarity determining regions by amino acid sequence analysis and structural homology modeling. The 19 IgG_1 rhMAbs (MAbs A-1, B-1, C-1, D-1, and E to S) and all of the IgG_2 and IgG_4 rhMAbs are classified as κ IgG antibodies. The four rhMAbs from MAb T to MAb W consist of λ light chains, and these light-chain constant regions are classified as IGLC3, IGLC1, IGLC2, and IGLC1, respectively, according to the international ImMunoGeneTics (IMGT) nomenclature rules [20, 21]. The germline families of the V_H and light chain variable regions (V_L regions) for each rhMAb

classified by the IMGT rules are also listed in Table 2.1.

Table 2.1.
Physicochemical properties of rhMAbs and retention time in hydroxyapatite chromatography by NaPi or NaCl gradient elution

rhMAb	Subclass	Type of light chain	Germline family of V_H region[a)]	Germline family of V_L region[a)]	Binding site of *N*-glycans	C_{NaPi}, NaPi gradient (mM)[b)]	C_{NaCl}, NaCl gradient (mM)[c)]
MAb A-1	IgG_1	κ	IGHV6	IGKV1	C_H2	308	685
MAb A-2	IgG_2	κ	IGHV6	IGKV1	C_H2	243	394
MAb A-4	IgG_4PE[d)]	κ	IGHV6	IGKV1	C_H2	275	1023
MAb B-1	IgG_1	κ	IGHV1	IGKV4	C_H2	280	623
MAb B-2	IgG_2	κ	IGHV1	IGKV4	C_H2	196	373
MAb B-4	IgG_4PE[d)]	κ	IGHV1	IGKV4	C_H2	242	1005
MAb C-1	IgG_1	κ	IGHV1	IGKV1	C_H2	253	591
MAb C-2	IgG_2	κ	IGHV1	IGKV1	C_H2	139	303
MAb C-4	IgG_4	κ	IGHV1	IGKV1	C_H2	202	565
MAb D-1	IgG_1	κ	IGHV1	IGKV3	V_H, C_H2[f)]	190	540
MAb D-2	IgG_2	κ	IGHV1	IGKV3	V_H, C_H2[f)]	99	264
MAb D-4	IgG_4	κ	IGHV1	IGKV3	V_H, C_H2[f)]	125	496
MAb E	IgG_1	κ	IGHV1	IGKV1	C_H2	242	624
MAb F	IgG_1	κ	IGHV3	IGKV1	C_H2	233	659
MAb G	IgG_1	κ	IGHV3	IGKV1	C_H2	271	656
MAb H	IgG_1	κ	IGHV3	IGKV1	C_H2	254	632
MAb I	IgG_1	κ	IGHV3	IGKV3	C_H2	289	644
MAb J	IgG_1	κ	IGHV3	IGKV6	C_H2	250	637
MAb K	IgG_1	κ	IGHV3	IGKV6	C_H2	275	692
MAb L	IgG_1	κ	IGHV4	IGKV3	C_H2	241	655
MAb M	IgG_1	κ	IGHV4	IGKV3	C_H2	248	689
MAb N	IgG_1	κ	IGHV4	IGKV3	C_H2	239	680
MAb O	IgG_1	κ	IGHV4	IGKV3	C_H2	274	708
MAb P	IgG_1	κ	IGHV4	IGKV3	C_H2	257	667
MAb Q	IgG_1	κ	IGHV4	IGKV3	C_H2	262	638
MAb R	IgG_1	κ	IGHV4	IGKV1	C_H2	210	658
MAb S	IgG_1	κ	IGHV5	IGKV1	C_H2	249	665
MAb T	IgG_1	λ	IGHV1	IGLV1	C_H2	203	517
MAb U	IgG_1	λ	IGHV3	IGLV7	C_H2	223	524
MAb V	IgG_1	λ	IGHV7	IGLV3	C_H2	176	394
MAb W	IgG_1	λ	IGHV3	IGLV1	C_H2	242	487
MAb 1	IgG_4	κ	IGHV3	IGKV3	C_H2	211	655
MAb 2	IgG_4P[e)]	κ	IGHV4	IGKV3	C_H2	210	673
MAb 3	IgG_4PE[d)]	κ	IGHV3	IGKV1	C_H2	188	1014
MAb 4	IgG_4PE[d)]	κ	IGHV3	IGKV1	C_H2	190	1011
MAb 5	IgG_4PE[d)]	κ	IGHV4	IGKV1	C_H2	229	877
MAb 6	IgG_4PE[d)]	κ	IGHV4	IGKV3	C_H2	201	963

a) Germline family was determined according to the immunogenetics nomenclature rules [20, 21].

b) Peak Na^+ concentration in hydroxyapatite chromatography by NaPi gradient elution [13].

c) Peak NaCl concentration in hydroxyapatite chromatography by NaCl gradient elution with 5 mM NaPi in the gradient buffers.

d) Ser228Pro and Leu235Glu mutated forms of the IgG_4 heavy chain [19].

e) Ser228Pro mutated form of the IgG_4 heavy chain [18].

f) Presence of *N*-glycan in the V_H region was confirmed by sugar-chain analysis.

2.3.2. Instrumentation and materials for chromatography experiments

Chromatography experiments were performed on an Alliance HPLC workstation (Waters, Milford, MA, USA). Ceramic hydroxyapatite type II with an average bead size diameter of 20 μm (BioRad Laboratories, Hercules, CA, USA) was used as the chromatography medium, and was packed into a glass column of 3 mm internal diameter and 50 mm height (Kyoshin Kogyo, Tokyo, Japan). Sodium phosphate dibasic dodecahydrate (Junsei Chemical Co. Ltd., Tokyo, Japan), sodium phosphate monobasic dihydrate (Kokusan Chemical Co. Ltd., Tokyo, Japan), sodium chloride (Tomita Pharmaceutical Co. Ltd., Tokushima, Japan), HEPES (Dojindo Laboratories, Kumamoto, Japan), sodium hydroxide (Kokusan Chemical Co. Ltd.) and purified water were used to prepare the chromatography buffers. All reagents used were of analytical or pharmaceutical grade.

2.3.3. Hydroxyapatite chromatography by the NaCl gradient elution method

Both 5 mM NaPi, pH 6.8 (buffer A) and 2 M NaCl in 5 mM NaPi, pH 6.8 (buffer B) were used as the equilibration and elution buffers, respectively, for the NaCl gradient elution method with NaPi in the chromatography buffers. For the NaCl gradient elution method with HEPES in the chromatography buffers, 5 mM HEPES, pH 6.8 (buffer C) and 2 M NaCl in 5 mM HEPES, pH 6.8 (buffer D) were used. The flow rate was 0.35 mL/min. Samples were loaded on the hydroxyapatite column at 0.035 mg rhMAb/mL hydroxyapatite. The sample injection volume was 50 μL. After washing the column with buffer A or buffer C for 5 min, elution was performed for 30 min with a linear gradient from buffer A to buffer B, or from buffer C to buffer D, followed by a 2-min step elution with buffer B or buffer D. The column was regenerated with 400 mM NaPi, pH 6.8 (buffer E) at 0.7 mL/min for 13 min. Chromatographic runs were performed at 25°C, and the column effluent was monitored at 215 nm and 280 nm. The baseline absorbance at 215 nm increased during gradient elution, and the correlation formula between run time and NaCl concentration of the column effluent could be calculated. The C_{NaCl} value for each rhMAb was determined using the correlation formula and peak retention time. Chromatography experiments for each rhMAb sample were conducted in duplicate, and

the average C_{NaCl} values were used for interpretation.

2.3.4. Hydroxyapatite chromatography by the NaPi gradient elution method

The hydroxyapatite column was equilibrated with 5 mM NaPi, pH 6.8 (buffer A). The flow rate was 0.35 mL/min. Samples were loaded onto the column at 0.035 mg rhMAb/mL hydroxyapatite. The sample injection volume was 50 µL. After washing the column with buffer A for 5 min, elution was performed for 30 min with a linear gradient, from buffer A to 400 mM NaPi, pH 6.8 (buffer E). The column was regenerated with buffer E for 2 min. Chromatographic runs were performed at 25°C, and the column effluent was monitored at 280 nm.

2.4. Results and Discussion

2.4.1. Hydroxyapatite chromatography of 37 rhMAbs performed by NaCl gradient elution with NaPi in the chromatography buffers

Chromatography experiments by NaCl gradient elution were performed using the 37 rhMAbs in the presence of 5 mM NaPi in the binding and elution buffers to correlate the retention times of rhMAbs (C_{NaCl}) with their structures. Classification of the rhMAbs is shown in Table 2.1, according to subclass, type of light chain, and germline family of the variable regions, and includes 19 κ IgG_1, 4 λ IgG_1, 4 κ IgG_2, and 10 κ IgG_4 antibodies. Table 2.1 also includes peak sodium ion concentration values in NaPi gradient hydroxyapatite chromatography obtained in our previous study [13]. According to the inserted point mutations in the hinge region and the second heavy chain constant region (C_H2 region), 10 κ IgG_4 rhMAbs can be further classified into three groups of antibodies: 3 IgG_4, 1 IgG_4P, and 6 IgG_4PE. MAbs D-1, D-2, and D-4 contain an *N*-glycan structure between the second and third complementarity determining regions. The 12 rhMAbs from MAb A-1 to MAb D-4 comprise four sets of variable domain-identical antibodies. Thus, the rhMAbs of each group have identical amino acid sequences in the variable regions, and only differ by subclass (IgG_1, IgG_2, or IgG_4 or IgG_4PE). Wide variation found in the germline family of both V_H and V_L regions in the selected rhMAbs ensures

the diversity required in the present study (Table 2.1).

From a comparison of the C_{NaCl} values of each rhMAb sample, an apparent relationship could be observed between the C_{NaCl} value and the heavy chain subclass for the κ IgG rhMAbs, except for MAbs D-1, D-2, and D-4 (Fig. 2.1). The retention times were broadly classified into three groups as follows: (1) κ IgG_2, (2) κ IgG_1, κ IgG_4 and κ IgG_4P, and (3) κ IgG_4PE. Additionally, the elution order of MAbs C-1 vs. C-4 and MAbs D-1 vs. D-4 showed that κ IgG_4 rhMAb eluted slightly earlier than its κ IgG_1 subclass isotype. Although the C_{NaCl} value varied among the subclass-identical rhMAbs possessing the same type of light chain (e.g., κ IgG_1 rhMAbs), this variation was not large compared with the variation among the subclass isotypes (e.g., MAbs A-1, A-2, and A-4). With respect to the contribution of light chain types, the λ IgG_1 rhMAbs eluted earlier than the κ IgG_1 counterparts. As shown in Fig. 2.1, IgG_2 rhMAbs exhibited the earliest elution time compared with IgG_1 and IgG_4 rhMAbs, which is in agreement with the results of Wensel et al. [10]. Although they report that IgG_1 and IgG_4 humanized MAbs were indistinguishable in their binding to hydroxyapatite, we found that κ IgG_4 rhMAbs eluted slightly earlier than their κ IgG_1 subclass isotypes. This is because we utilized the subclass isotypes with the same Fab region (MAbs C or MAbs D). With regard to the light chain types, the λ IgG_1 rhMAbs tended to elute earlier than the κ IgG_1

counterparts. Wensel et al concluded that there were no consistent trends in the binding between κ IgG and λ IgG MAbs [10]; however, their data indicated a similar tendency under the conditions of the present study (NaPi concentration: 5 mM, pH6.8). Obviously, the κ IgG_4PE rhMAbs showed the latest retention times, despite the fact that the retention times of κ IgG_4PE and κ IgG_4 rhMAbs in NaPi gradient hydroxyapatite chromatography did not show any difference due to the mutation [13], and that the retention times in the NaPi gradient chromatography showed a common positive linearity with the number of surface distributed basic amino acid residues [13]. MAbs D-1, D-2, and D-4, which have *N*-glycan structures in their V_H regions, eluted the earliest among their subclass-identical κ IgG rhMAbs, probably due to interference by binding to hydroxyapatite. The same tendency was observed in the retention behavior in NaPi gradient chromatography [13], which showed that these rhMAbs did not meet the linear trend between retention times and basic residues of rhMAbs without *N*-glycan in the V_H regions.

From these results, the retention behavior of rhMAbs in the NaCl gradient hydroxyapatite chromatography with 5 mM NaPi in the chromatography buffers could be classified according to subclass and type of light chain.

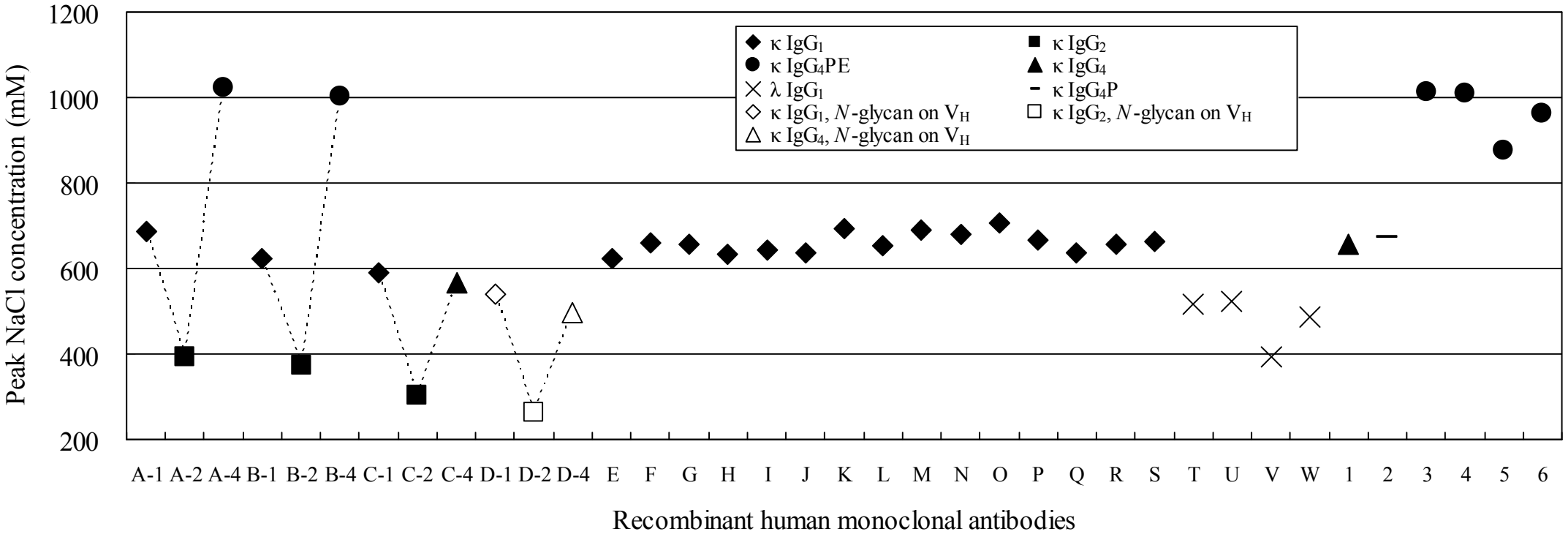

Fig. 2.1. Peak NaCl concentration values of rhMAbs in hydroxyapatite chromatography obtained by NaCl gradient elution with 5 mM NaPi in the chromatography buffers. Column: Ceramic hydroxyapatite type II, 20-μm beads, 3-mm diameter × 50-mm length; binding buffer: 5 mM NaPi, pH 6.8; elution buffer: 2 M NaCl in 5 mM NaPi, pH 6.8; elution: 30 min, with a linear gradient from the binding buffer to the elution buffer at a flow rate of 0.35 mL/min; injection: 0.035 mg rhMAb/mL hydroxyapatite.

2.4.2. NaCl gradient elution without NaPi in the chromatography buffers

Chromatography experiments by NaCl gradient elution methods without NaPi in the gradient buffers were performed for the 20 rhMAbs (MAbs A-1 to D-4, T to W, 1, 2, 5, and 6) to further clarify the retention behavior of rhMAbs. The method was the same as that used for the experiments in section 2.4.1 except for the gradient buffers: 5 mM HEPES, pH 6.8, was used for the binding buffer, and 2 M NaCl in 5 mM HEPES, pH 6.8 for the elution buffer. The C_{NaCl} values obtained are compared in Fig. 2.2.

The results show that only the κ IgG_2 and κ IgG_4 rhMAbs were eluted by the NaCl gradient elution without NaPi. On the other hand, κ IgG_1, κ IgG_4PE, and λ IgG_1 rhMAbs were not eluted even with 2 M NaCl, and were finally eluted in the regeneration step with 400 mM NaPi, pH 6.8. Although the C_{NaCl} values of κ IgG_1 and κ IgG_4 rhMAbs were similar (but to be exact, κ IgG_4 < κ IgG_1) in NaCl gradient hydroxyapatite chromatography with 5 mM NaPi in the gradient buffers, only the κ IgG_4 rhMAbs were eluted by the NaCl gradient elution without NaPi. The C_{NaCl} values of all subclasses apparently increased by removing the low concentration NaPi from the chromatography buffers, indicating that metal-affinity interactions are involved in the adsorption for all subclasses. Although metal-affinity interactions were not thought to be affected by

conductivity, Gagnon et al. suggested that weak metal-affinity interactions could be broken by increasing conductivity [22]. Thus, it can be considered that the metal-affinity interactions of IgG_2 and IgG_4 rhMAbs are relatively weak compared with those of IgG_1 and IgG_4PE rhMAbs.

The elution of κ IgG_4 rhMAbs but not λ IgG_1 rhMAbs by NaCl in the absence of 5 mM NaPi suggests stronger metal-affinity interactions of λ IgG_1 rhMAbs than κ IgG_4 rhMAbs; however, the λ IgG_1 rhMAbs tended to elute earlier than the κ IgG_4 rhMAbs by NaCl gradient elution with NaPi (Figs. 2.1 and 2.2). These results suggest that some other interaction mechanisms would contribute to the retention behavior in the NaCl gradient elution mode with 5 mM NaPi.

Together with the results described in sections 2.4.1 and 2.4.2, it is suggested that each heavy chain subclass or light chain subclass can be separated by hydroxyapatite chromatography when an appropriate buffer composition is selected.

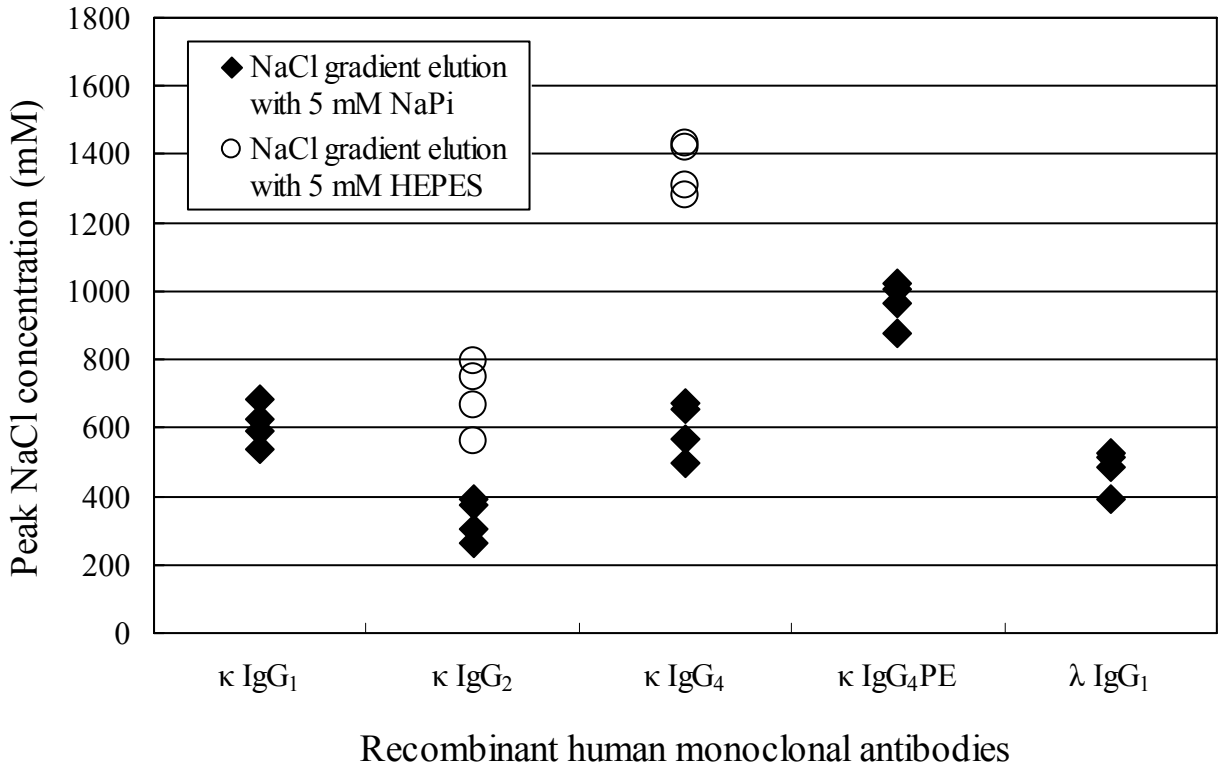

Fig 2.2. Plot of the retention times of 20 rhMAbs (MAbs A-1 to D-4, T to W, 1, 2, 5, and 6) in hydroxyapatite chromatography obtained by NaCl gradient elution with and without NaPi in the gradient buffers. Column: Ceramic hydroxyapatite type II, 20-μm, 3-mm diameter × 50-mm length; binding buffer (black diamond): 5 mM NaPi, pH 6.8, (white circle): 5 mM HEPES, pH 6.8; elution buffer (black diamond): 2 M NaCl in 5 mM NaPi, pH 6.8, (white circle): 2 M NaCl in 5 mM HEPES, pH 6.8; elution: a 30 min linear gradient from the binding buffer to the elution buffer at a flow rate of 0.35 mL/min; Regeneration: 400 mM NaPi, pH 6.8 at 0.7 mL/min for 13 min; injection: 0.035 mg rhMAb/mL hydroxyapatite. The κ IgG_1, κ IgG_4PE, and λ IgG_1 rhMAbs were not eluted even with 2 M NaCl, and were finally eluted in the regeneration step with 400 mM NaPi.

2.4.3. Interaction of the glutamate residue in IgG_4PE with hydroxyapatite

IgG_4PE rhMAb has two point mutations: Ser228Pro in the hinge region and Leu235Glu in the C_H2 region. The C_{NaCl} values of the IgG_4PE rhMAbs in the presence of 5 mM NaPi are clearly higher than the C_{NaCl} values of the IgG_4 and IgG_4P rhMAbs (Fig. 2.1). To investigate the effects of Glu-235 on the retention behavior, we compared the chromatograms of κ IgG_4P and κ IgG_4PE rhMAbs by NaPi gradient elution and by NaCl gradient elution with 5 mM NaPi (Figs. 2.3A and 2.3B). The amino acid sequences of the two rhMAbs only differ at the residue at position 235 in the heavy chain. These two rhMAbs eluted at exactly the same retention time in the NaPi gradient elution (Fig. 2.3A); however, IgG_4PE rhMAb eluted apparently later than the IgG_4P rhMAb in the NaCl gradient elution (Fig. 2.3B). Since the coordination of closely located carboxyl groups on glutamate or aspartate residues are reported to generate metal-affinity interactions [6–9], it was suggested that the Glu-235 residues of IgG_4PE antibodies were involved in forming strong metal-affinity interactions and contributed to the retention behavior. The Glu-235 residues, which are located in the C_H2 regions, are adjacent to the disulfide bridge in the hinge region. Although there is limited 3D structural information on this region of human IgG_4 proteins, two negatively charged amino acid residues are

believed to be located close to the Glu-235 residue: a Glu residue at position 233 and another Glu residue at position 235 on the paired C_H2 region. The coordination of these Glu residues is expected to generate one or two metal-affinity interactions between IgG_4PE rhMAb and hydroxyapatite.

The peak retention times of the IgG_4PE and the IgG_4P rhMAb were completely identical by NaPi gradient elution (Fig. 2.3A). Additionally, in our previous study regarding NaPi gradient elution, the retention times of the κ IgG_4PE and κ IgG_4 rhMAbs showed a common positive linearity with the number of surface distributed basic amino acid residues [13]. These results indicate that the generated metal affinity interactions by Glu-235 do not influence the retention behavior in the NaPi gradient elution.

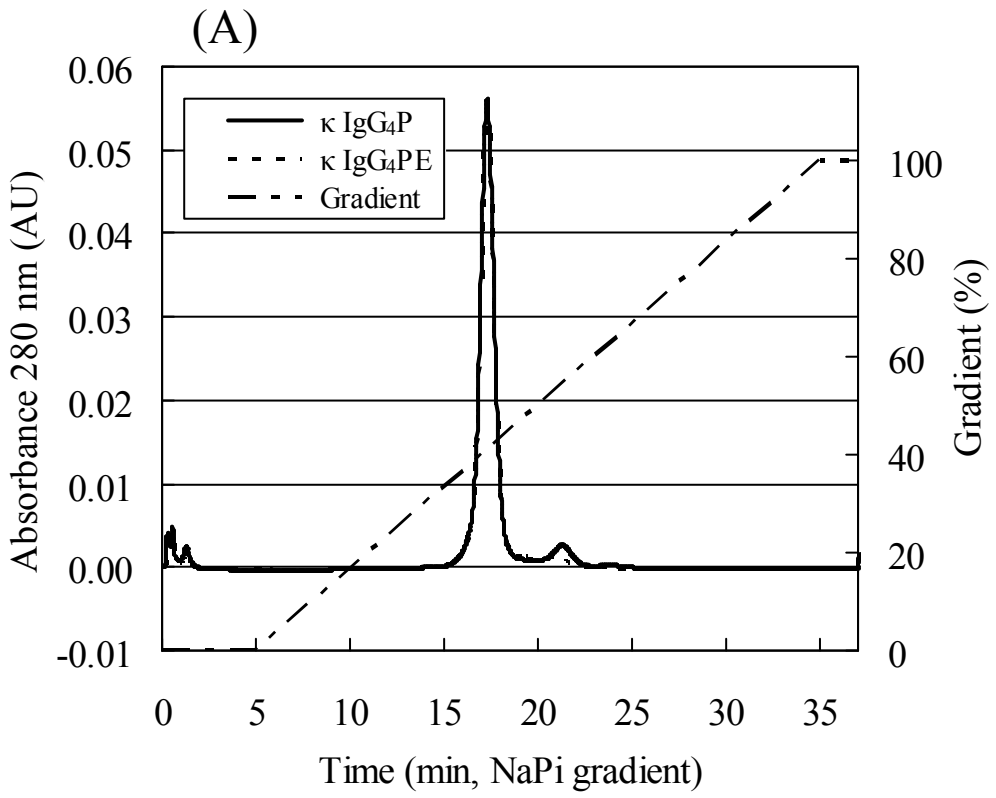
(A)
κ IgG4P
κ IgG4PE
Gradient
Absorbance 280 nm (AU)
Gradient (%)
Time (min, NaPi gradient)
0.06
0.05
0.04
0.03
0.02
0.01
0.00
-0.01
100
80
60
40
20
0
0
5
10
15
20
25
30
35

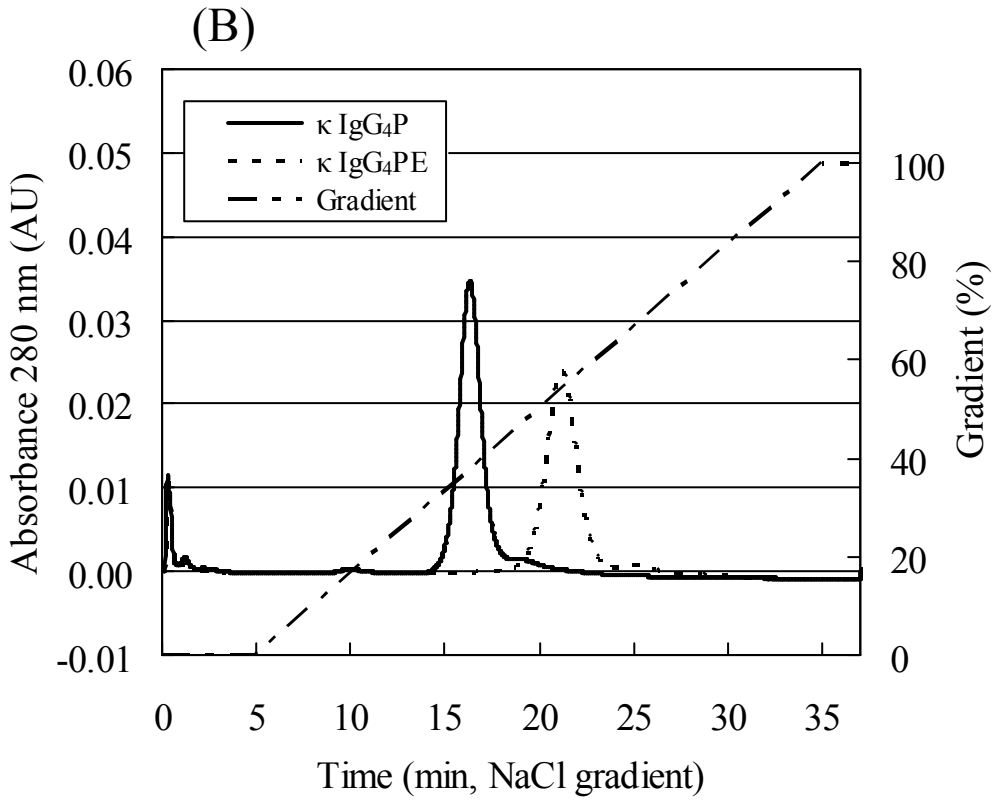
(B)
κ IgG4P
κ IgG4PE
Gradient
Absorbance 280 nm (AU)
Gradient (%)
Time (min, NaCl gradient)
0.06
0.05
0.04
0.03
0.02
0.01
0.00
-0.01
100
80
60
40
20
0
0
5
10
15
20
25
30
35

Fig 2.3. Hydroxyapatite chromatograms of a κ IgG_4P rhMAb and its Leu235Glu mutated form (κ IgG_4PE rhMAb) obtained by (A) NaPi gradient elution, and (B) NaCl gradient elution with 5 mM NaPi in the gradient buffers. Column: Ceramic hydroxyapatite type II, 20-μm, 3-mm diameter × 50-mm length; binding buffer: 5 mM NaPi, pH 6.8; elution buffer (A): 2 M NaCl in 5 mM NaPi, pH 6.8, (B): 400 mM NaPi, pH 6.8; elution: a 30 min linear gradient from the binding buffer to the elution buffer at a flow rate of 0.35 mL/min; injection: 0.035 mg rhMAb/mL hydroxyapatite. The small trailing peak or shoulder appearing after the main peak is considered an antibody aggregate [4, 5, 22].

2.4.4. Comparison of retention times of NaCl elution with those of NaPi elution

Figure 2.4 shows the plots of the peak NaCl concentration against the peak NaPi concentration for all 37 rhMAbs. The retention time values by NaPi gradient elution (Table 2.1) were obtained in our previous study [13]. Positive correlation was observed between the retention times by these two gradient modes except for IgG_4PE rhMAbs, which showed apparently higher retention time values by NaCl gradient elution compared with other subclasses.

The results in section 2.4.3 indicated that the replaced amino acid residue of Glu-235 in κ IgG_4PE rhMAbs does not greatly affect the retention time in NaPi gradient elution, although the generated metal affinity interactions on the κ IgG_4PE rhMAbs by the alteration of Leu235Glu are supposed to be the strongest. Thus, it is suggested that the major separation mode of the NaPi gradient hydroxyapatite chromatography is cation-exchange, although both phosphoryl cation exchange interactions and metal-affinity interactions contribute to the binding of rhMAbs to hydroxyapatite.

In the NaCl gradient hydroxyapatite chromatography with 5 mM NaPi, the phosphoryl cation exchange interactions may affect the retention times of rhMAbs because the retention times of these rhMAbs by NaCl and NaPi gradient elutions showed a positive correlation (Fig. 2.4). However, the retention times of IgG_4PE rhMAbs were markedly higher than those of other subclasses. Furthermore, the correlation between retention time and the number of surface-distributed basic amino acid residues observed in the elution with NaPi gradient [13], was not observed in the present elution with the NaCl gradient with 5mM NaPi (data not shown). From these observations, interaction mechanisms other than the phosphoryl cation exchange interactions—most probably metal affinity interactions—must affect the retention behavior cooperatively. Compared to the NaPi gradient elution, the contribution of the metal affinity interaction is greater in

the NaCl gradient elution. This interpretation is in good agreement with previous publications that consider the cooperation of both interaction mechanisms for whole antibody molecules [22], and that found that calcium-metal-affinity interactions of antibodies are affected by increasing conductivity [11, 22]. In IgG_4PE rhMAbs, the metal affinity interaction is supposed to be dominant because these rhMAbs apparently did not meet the linear trends indicated in Fig. 2.4.

Regarding κ IgG and λ IgG rhMAbs, the λ IgG_1 rhMAbs eluted earlier than κ IgG_1 rhMAbs (Fig. 2.1). λ IgG has been known to have conformational flexibility between the variable and constant domains. Such a structural difference may influence accessibility of the antibodies to hydroxyapatite.

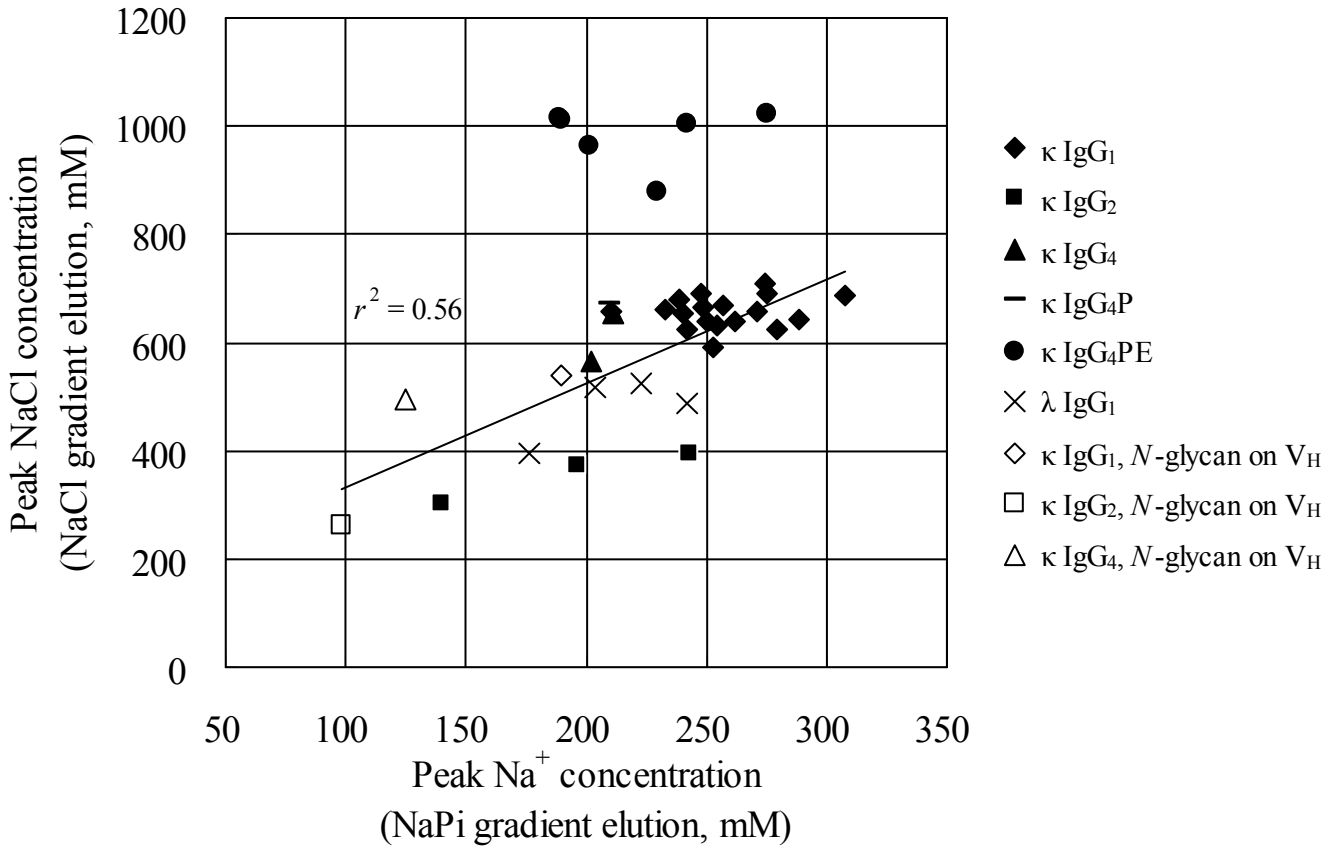

Fig 2.4. Comparison of retention times by NaPi gradient elution and NaCl gradient elution with 5 mM NaPi. The values obtained are presented in Table 1. Column: Ceramic hydroxyapatite type II, 20-μm, 3-mm diameter × 50-mm length; binding buffer: 5 mM NaPi, pH 6.8; elution buffer (NaPi gradient): 400 mM NaPi, pH 6.8, (NaCl gradient): 2 M NaCl in 5 mM NaPi, pH 6.8; elution: a 30 min linear gradient from the binding buffer to the elution buffer at a flow rate of 0.35 mL/min; injection: 0.035 mg rhMAb/mL hydroxyapatite. The correlation coefficient was calculated using the data, except that for the κ IgG_4PE rhMAbs.

2.5. Concluding remarks

In the hydroxyapatite chromatography of rhMAbs by NaCl gradient elution in the presence of 5 mM NaPi, it was suggested that the retention time could be classified by subclass and type of light chain. In the absence of NaPi in the chromatography buffer, IgG_1 and IgG_4 rhMAbs were not eluted even with 2M NaCl. Retention time is supposed to be affected by phosphoryl cation exchange interactions under a buffer composition with 5 mM NaPi in the gradient buffer. However, the separation mode is not the single ion exchange; other interaction mechanisms of metal affinity interaction would also be involved. That is, the cation exchange and metal affinity interactions affect the retention behavior cooperatively. The contribution of metal affinity interactions is greater in NaCl gradient hydroxyapatite chromatography than in NaPi gradient elution chromatography. Furthermore, for IgG_4PE rhMAbs, metal-affinity interactions would be dominated in hydroxyapatite chromatography with NaCl gradient elution.

Hydroxyapatite chromatography is a powerful method for purifying MAbs. Understanding the retention behavior of the antibodies required is useful for the design of MAb purification methods. Thus, the different elution propensities of MAbs that depend on the MAb structures (heavy chain subclasses, light chain isotypes, and the number of surface distributed basic amino acid residues) and gradient elution buffers

(NaPi or NaCl), as discovered in our previous [13] and present studies should be informative for the efficient purification-process development of rhMAbs.

2.6. References

[1] Tiselius, A., Hjertén, S., Levin, Ö., *Arch. Biochem. Biophys.* 1956, *65*, 132-155.

[2] Gagnon, P., *Purification Tools for Monoclonal Antibodies*, Validated Biosystems, San Clemente, U.S.A. 1996, pp. 87-102.

[3] Horenstein, A. L., Crivellin, F., Funaro, A., Said, M., Malavasi, F., *J. Immunol. Methods* 2003, *275*, 99-112.

[4] Gagnon, P., Ng, P., Zhen, J., Aberin, C., He, J., Mekosh, H., Cummings, L., Zaidi, S., Richieri, R., *Bioprocess Int.* 2006, *4*, 50-60.

[5] Gagnon, P., *N. Biotechnol.* 2009, *25*, 287-293.

[6] Bernardi, G., *Methods Enzymol.* 1973, *27*, 471-479.

[7] Gorbunoff, M. J., *Anal. Biochem.* 1984, *136*, 425-432.

[8] Gorbunoff, M. J., *Anal. Biochem.* 1984, *136*, 433-439.

[9] Gorbunoff, M. J., Timasheff, S. N., *Anal. Biochem.* 1984, *136*, 440-445.

[10] Wensel, D. L., Kelley, B. D., Coffman, J. L., *Biotechnol. Bioeng.* 2008, *100*, 839-854.

[11] Schubert, S., Freitag, R., *J. Chromatogr. A* 2009, *1216*, 3831-3840.

[12] Gagnon, P., Cheung, C., Yazaki, P. J., *J. Immunol. Methods* 2009, *342*, 115-118.

[13] Nakagawa, T., Ishihara, T., Yoshida, H., Yoneya, T., Wakamatsu, K., Kadoya, T., *J.*

Sep. Sci. 2009, *33*, 1-9.

[14] Ishida, I., Tomizuka, K., Yoshida, H., Tahara, T., Takahashi, N., Ohguma, A., Tanaka, S., Umehashi, M., Maeda, H., Nozaki, C., Halk, E., Lonberg, N., *Cloning Stem Cells* 2002, *4*, 91-102.

[15] Carter, P. J., *Nat. Rev. Immunol.* 2006, *6*, 343-357.

[16] Hober, S., Nord, N., Linhult, M., *J. Chromatogr. B* 2007, *848*, 40-47.

[17] Kabat, E. A., Wu, T. T., Perry, H. M., Gottesman, K. S., Foeller, C., *Sequences of Proteins of Immunological Interest (5th ed.)*, Public Health Service, National Institutes of Health, Bethesda, U.S.A. 1991.

[18] Angal, S., King, D. J., Bodmer, M. W., Turner, A., Lawson, A. D. G., Roberts, G., Pedley, B., Adair, J. R., *Mol. Immunol.* 1993, *30*, 105-108.

[19] Reddy, M. P., Kinney, C. A. S., Chaikin, M. A., Payne, A., Fishman-Lobell, J., Tsui, P., Monte, P. R. D., Doyle, M. L., Brigham-Burke, M. R., Anderson, D., Reff, M., Newman, R., Hanna, N., Sweet, R. W., Truneh, A., *J. Immunol.* 2000, *164*, 1925-1933.

[20] WHO-IUIS Nomenclature SubCommittee for Immunoglobulins and T cell receptors report, *13th International Congress of Immunology*, Rio de Jaeiro, Brazil 2007.

[21] Lefranc, M. P., Pommié, C., Kaas, Q., Duprat, E., Bosc, N., Guiraudou, D., Jean, C.,

Ruiz, M., Piédade, I. D., Rouard, M., Foulquier, E., Thouvenin, V., Lefranc, G., *Dev. Comp. Immunol.* 2005, *29*, 185-203.

[22] Gagnon, P., Cheung, C., Yazaki, P. J., *J. Sep. Sci.* 2009, *32*, 3857-3865.

CONCLUSIONS

Hydroxyapatite chromatography is one of the efficient chromatography tools for rhMAbs production. In this study, retention behavior of various rhMAbs in hydroxyapatite chromatography by each of NaPi and NaCl gradient elution methods was investigated according to the physicochemical properties of the antibody structures.

The following features are the principal results obtained in the present study:

1. NaPi gradient elution:

(i) The structure of both constant and variable regions affects the retention time independently.

(ii) The number of positively charged amino acid residues in the variable region, particularly in the heavy chain, correlates well with the retention behavior.

(iii) Among rhMAbs of same constant regions (subclass, type of light chains), the correlation is more pronounced when the surface accessibility of the positively charged amino acid residues are taken into consideration.

(iv) λ IgG rhMAbs tend to elute earlier than κ IgG rhMAbs when their subclass is identical.

(v) *N*-glycan structures on the V_H regions might inhibit the interaction.

(vi) The major separation mode is cation-exchange, although both phosphoryl cation

exchange interactions and metal-affinity interactions contribute to the binding of rhMAbs to hydroxyapatite.

(vii) Although *p*I value of protein is reported to show a positive correlation to the retention behavior in hydroxyapatite chromatography by NaPi elution, such a correlation for antibody was not observed in the present study.

2. NaCl gradient elution:

(i) The retention time can be classified by subclass and type of light chain.

(ii) λ IgG rhMAbs tend to elute earlier than κ IgG rhMAbs of the same subclass.

(iii) *N*-glycan structures on the V_H regions might inhibit the interaction.

(iv) The cation exchange and metal affinity interactions affect the retention behavior cooperatively.

(v) The contribution of metal affinity interactions is greater in the NaCl gradient elution chromatography than in NaPi gradient elution chromatography.

From these results, it was found that the retention behavior of human antibodies in hydroxyapatite chromatography can be classified according to the primary structure of the antibodies. Reliable prediction of the retention time in column chromatography

purification according to readily obtained information, such as the amino acid sequence of target MAbs, can serve as a guide for the optimization of the elution buffer conditions as well as the estimation of purity levels, which will facilitate the development of purification processes. For example, by compiling preliminary information about the retention time of the impurities such as production cell-derived proteins, genomic DNA, and components of the cell culture media, the effect of removal of those impurities through the purification of the target MAbs can be predicted. Therefore, under the conditions of heated competition in a growing market of antibody therapy, these findings will help to minimize the development period in the early stage of process development.

ACKNOWLEDGEMENTS

First of all, I would like to thank Professor Kaori Wakamatsu for giving me an opportunity to publish this doctoral work, and for always teaching me how to approach logically.

I would also like to thank Professor Toshihiko Kadoya for making a number of valuable suggestions over the whole stage of the present work, and for motivating me to keep going.

I would like to acknowledge Dr. Takashi Ishihara, Hideaki Yoshida, and Takashi Yoneya for the advising and coordination of this work throughout these 3 years.

My gratitude also goes to Manami Kinoe for her technical assistance of the purification and analysis in this study.

I would like to thank Dr. Eiji Mori, and Yuji Yamazaki for providing me their valuable rhMAb samples.

I also acknowledge gratefully Dr. Masayoshi Tsukahara, Kazuo Kobayashi, and Dr. Kousuke Kuroda for their many discussions and scientific inspirations while preparing the publications.

I also thank the support of Kyowa Hakko Kirin Co., Ltd. for giving me this opportunity.

I would like to thank my wife, Momoko, and my children, Mioko and Rikako for their loves and supports during this extremely difficult time.

I recognize this work would never be accomplished without their kind help.

Taishiro Nakagawa

LIST OF ACCOMPLISHMENTS

1. Journal of Separation Science, 2010, 33, 37-45

Taishiro Nakagawa[1,2], Takashi Ishihara[1], Hideaki Yoshida[3], Takashi Yoneya[4], Kaori Wakamatsu[2], and Toshihiko Kadoya[1,5]

[1]Bio Process Research and Development Laboratories, Production Division, Kyowa Hakko Kirin Co., Ltd., Gunma, Japan
[2]Department of Biological and Chemical Engineering, Faculty of Engineering, Gunma University, Gunma, Japan
[3]Antibody Research Laboratories, Research Divi sion, Kyowa Hakko Kirin Co., Ltd., Gunma, Japan
[4]Fuji Research Park, Research Division, Kyowa Hakko Kirin Co., Ltd., Shizuoka, Japan
[5]Department of Biotechnology, Faculty of Engineering, Maebashi Institute of Technology, Gunma, Japan

"Relationship between human IgG structure and retention time in hydroxyapatite chromatography with sodium-phosphate gradient elution"

2. Journal of Separation Science, 2010, 33, 2045-2051

Taishiro Nakagawa[1,2], Takashi Ishihara[1], Hideaki Yoshida[3], Takashi Yoneya[4], Kaori Wakamatsu[2], and Toshihiko Kadoya[1,5]

[1]Bio Process Research and Development Laboratories, Production Division, Kyowa Hakko Kirin Co., Ltd., Gunma, Japan

[2]*Department of Biological and Chemical Engineering, Faculty of Engineering, Gunma University, Gunma, Japan*
[3]*Antibody Research Laboratories, Research Division, Kyowa Hakko Kirin Co., Ltd., Gunma, Japan*
[4]*Fuji Research Park, Research Division, Kyowa Hakko Kirin Co., Ltd., Shizuoka, Japan*
[5]*Department of Biotechnology, Faculty of Engineering, Maebashi Institute of Technology, Gunma, Japan*

"Relationship between human IgG structure and retention time in hydroxyapatite chromatography with sodium-chloride gradient elution"

3. Poster presentation at 21st International Symposium, Exhibit & Workshops on Preparative / Process Chromatography, June 15 - 18, 2008, San Jose, CA, USA

Taishiro Nakagawa [a, b], Takashi Ishihara [b], Kaori Wakamatsu [a], and Toshihiko Kadoya [b]

[a] *Department of Biological and Chemical Engineering, Faculty of Engineering, Gunma University, Gunma, Japan*
[b] *CMC R&D Laboratories, Production Division, Kirin Pharma Company, Limited, Gunma, Japan*

"Retention behavior of recombinant human monoclonal antibodies in hydroxyapatite chromatography"